12 TECHNICOLOR

12.1 Introduction

Georges Azuelos and Francesco Sannino

A number of possible generalizations of the standard model have been conceived. Such extensions are introduced on the basis of one or more guiding principles or prejudices.

By invoking the absence of fundamental scalars in Nature one is led to construct theories in which the electroweak symmetry breaks via a fermion bilinear condensate. The Higgs sector of the Standard Model becomes an effective description of a more fundamental fermionic theory. This is similar to the Ginzburg-Landau theory of superconductivity. If the force underlying the fermion condensate driving electroweak symmetry breaking is due to a strongly interacting gauge theory these models are termed technicolor. Here we will discuss the basic models and summarize experimental searches.

Technicolor, in brief, is an additional non-abelian and strongly interacting gauge theory augmented with (techni)fermions transforming under a given representation of the gauge group. The Higgs Lagrangian is replaced by a suitable new fermion sector interacting strongly via a fifth force (technicolor). Schematically:

$$L_{Higgs} \to -\frac{1}{4}F_{\mu\nu}F^{\mu\nu} + i\bar{Q}\gamma_\mu D^\mu Q \ , \tag{12.1}$$

where, to be as general as possible, we have left unspecified the underlying nonabelian gauge group and the associated technifermion representation. The characteristic scale of the new theory is expected to be less than or of the order of one TeV. The chiral-flavor symmetries of this theory, as for ordinary QCD, break spontaneously when the technifermion condensate $\bar{Q}Q$ forms. It is possible to choose the fermion charges in such a way that there is, at least, a weak left-handed doublet of technifermions and the associated right-handed one which is a weak singlet. The covariant derivative contains the new gauge field as well as the electroweak ones. The condensate spontaneously breaks the electroweak symmetry down to the electromagnetic and weak interactions. The Higgs is now interpreted as the lightest scalar field with the same quantum numbers of the fermion-antifermion composite field. The Lagrangian part responsible for the mass-generation of the ordinary fermions will also be modified since the Higgs particle is no longer an elementary object.

Models of electroweak symmetry breaking via new strongly interacting theories of technicolor type [1,2] are a mature subject (for recent reviews see [3,4]). One of the main difficulties in constructing such extensions of the standard model is the very limited knowledge about generic strongly interacting theories. This has led theorists to consider specific models of technicolor which resemble ordinary quantum chromodynamics and for which the large body of experimental data at low energies can be directly exported to make predictions at high energies.

To be able to make contact with experiments we need to introduce some of the phenomenological key players of technicolor theories. These are some of the hadronic states of the theory.

As we have already explained above, the technifl avor global symmetries, as for ordinary QCD, break spontaneously and technipions π_T will emerge as light states of the theory. Three of them become the longitudinal components of the W and Z gauge bosons. Since the quantum numbers of the remaining technipions are model dependent, it can happen that some carry weak charges and/or ordinary color charges. New sources of technifl avor symmetry breaking are needed to be able to provide large masses to the technipions. Vector mesons are relevant in QCD and their technivector cousins may equally play an important role for the technicolor theories. According to the underlying model, as for technipions, these technihadrons can also experience the color and electroweak force. A mass in the several hundred GeV range is expected.

The situation for the composite Higgs boson is more delicate. According to the common lore generic theories of composite Higgs contain large corrections with respect to the minimal standard model,

similar to those of a heavy elementary Higgs boson [5]. However, a heavy composite Higgs is *not* necessarily an outcome of strong dynamics [6–10]. Here we are not referring to models in which the Higgs is a quasi Goldstone boson [11], investigated recently in [12] (see Section 7).

In the analysis of QCD-like technicolor models information on the non-perturbative dynamics at the electroweak scale is obtained by simply scaling up QCD phenomenology to the electroweak energy scale. The Higgs particle is then mapped into the $q\bar{q}$ scalar partner of the pions in QCD. However, the scalars are a complicated sector of QCD (see the PDG - review dedicated to this sector of the theory). There is a growing consensus that the low lying scalar object, i.e. $f_0(600)$, needed to provide a good description of low energy pion pion scattering [13, 14] is not the chiral partner of the pions but is of four quark nature à la Jaffe [15, 16]. Recent arguments, based on taking the 't Hooft limit of a large number of colors N, also demonstrate that the low energy scalar is not of $q\bar{q}$ nature [17]. The natural candidate for the scalar partner of the ordinary pions is very heavy, i.e. it has a mass larger than one GeV. When transposed to the electroweak theory by simply taking the scaled pion decay constant F_π as the electroweak scale, one concludes that in technicolor theories with QCD-type dynamics the composite Higgs is very heavy, $m_H \sim 4\pi F_\pi$, of the order of the TeV scale. This implies that corrections are needed to compensate the effects of such a heavy Higgs in order not to be at odds with the electroweak precision measurements data. The presence of a heavy Higgs, however, does not exclude the possibility to observe a lighter and very broad techniscalar below the TeV region constructed with more than two technifermions in analogy with the $f_0(600)$ of QCD. For strongly interacting theories with non-QCD-like dynamics we are no longer guaranteed that the associated composite Higgs particle is heavy.

To generate standard model fermion masses in technicolor theories additional interactions are needed. Extended technicolor (ETC) models (Section 12.2), which couple technifermions to ordinary fermions [18], are an example of such interactions. Typically one imagines a very large gauge group in which color, flavor and technicolor are embedded simultaneously. Such a gauge group must then break to ordinary color and technicolor. The breaking of the ETC gauge group provides also masses to the ETC gauge bosons which are not part of the technicolor and color interactions. ETC massive gauge bosons and associated dynamics can lead to:

- a mass term for the standard model fermions,
- provide sufficiently large masses for some of the dangerously light technipions,
- technipions decaying into ordinary fermion pairs,
- couplings between fermions of different generations and hence to flavor-changing neutral currents.

Experimental constraints on interactions mediating flavor-changing neutral currents are obtained via the $K^0\ \bar{K}^0$ system [18]. These constraints for technicolor theories have been re-analyzed in [19] and found to be less restrictive. It turns out that the scale of ETC breaking must be of the order of hundreds to thousands of GeV. Such a high scale for the ETC interactions leads to very light technipions and quarks. This problem can be alleviated if the technifermion bilinear, whose condensate breaks the electroweak symmetry, can be dynamically enhanced. This is possible in theories in which the technicolor gauge coupling as function of the renormalization scale *walks* rather than run [20–24]. In Fig. 12.1 we provide a sketch of a typical walking coupling constant versus a standard running one. The enhancement of the condensate allows reasonable masses for light quarks and leptons, even for large ETC scales necessary to suppress flavor-changing neutral currents sufficiently well. However, to obtain the observed top mass, one can use the ETC type models presented in [19], or one must rely on additional dynamics, as in so-called non-commuting ETC models, where the ETC interaction does not commute with the electroweak interaction [25]. This last mechanism is similar in spirit to the topcolor assisted technicolor models [26, 27] which will be introduced later in the text.

Most of the models used in the literature have considered the technifermions in the fundamental representation of the gauge group. In this case one needs a very large number of technifermions, roughly of the order of $4N_{TC}$ with N_{TC} the number of technicolors, to achieve walking [28–31]. It is, in general, hard to reliably compute physical quantities in walking theories [4]. However attempts have been made

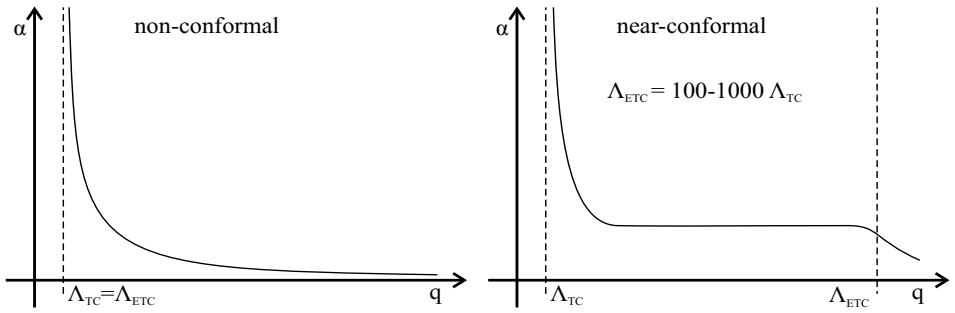

Fig. 12.1: Left Panel: A standard running behavior of a coupling constant in a generic asymptotically free theory. Right Panel: The walking behavior of the coupling constant when the number of flavors is near a conformal fixed point.

in the literature to provide an estimate of the S parameter [32]. One expects a reduced S parameter with respect to the naive one computed in perturbation theory [32–34].

Some of the previous problems can be ameliorated [8–10, 35] if one considers technifermions in higher dimensional representations of the technicolor gauge group. Here one achieves walking for a very small number of technifermions. Technicolor-like theories with fermions in higher dimensional representations of the gauge group have also been considered in the past [36–38]. For the walking type theories introduced in [8] it is argued that: i) The S-parameter is naturally small [9, 10]; ii) One has zero or a very small number of technipions [8]. A possible feature of these theories is that the resulting composite Higgs can be light with a mass of the order of 150 GeV. The phenomenology of these theories leads to interesting signatures as shown in Section 12.5.

It is instructive to examine the constraints from new precision measurements on the model presented in [10]. The model consists of two techniflavors in the adjoint representation of a two technicolor theory. A new lepton family is needed to have a consistent theory while the hypercharge needs not be the one of the standard model. In Fig. 12.2 the ellipse corresponds to the one sigma contour in the T$-$S plane. The central values for S$= +0.07 \pm 0.10$ and $T = +0.13 \pm 0.10$ have been taken from reference [39]. The black area bounded by parabolas corresponds to the region in the T$-$S plane obtained when varying the relative Dirac masses of the two new leptons. The point at T$= 0$ where the inner parabola meets the S axis corresponds to the contribution due solely to the technicolor theory. The electroweak parameters are computed perturbatively. Fortunately for walking technicolor theories the nonperturbative corrections further reduce the S parameter contribution [32, 33] and hence our estimates are expected to be rather conservative.

The figure clearly shows that the walking technicolor type theories are still viable models for dynamical breaking of the electroweak symmetry [40].

We stress that the S parameter problem, per se, can be alleviated in different ways [3, 41], also for walking technicolor theories with technifermions in the fundamental representation of the gauge group [42].

Although the ETC problem it not yet solved, some progress in building ETC models has been made in [19, 35] also with respect to the problem of generating neutrino masses [43]. The improvement with respect to earlier models is due to a better assignment of left and right-handed fermions to specific representations of a given ETC gauge group as well as of a better control over the walking dynamics [35]. Also the intragenerational mass splitting problem, especially the top-bottom mass one, has been recently re-investigated [19, 35, 44] with promising results. Particular care was payed in avoiding generating large corrections to the electroweak precision parameters.

There is the possibility that a top quark condensation may be responsible for part or all of the

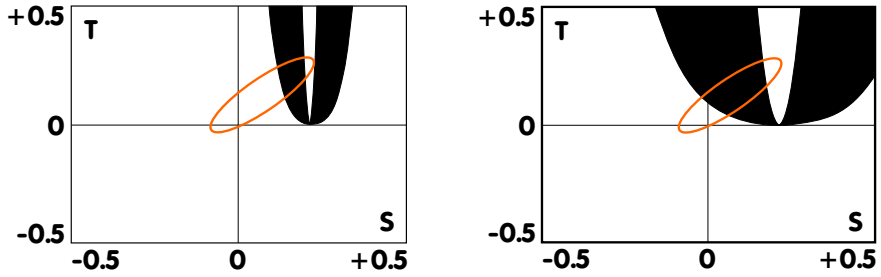

Fig. 12.2: Left Panel: The black shaded parabolic area corresponds to the accessible range of S and T for the extra neutrino and extra electron for masses from m_Z to $10m_Z$ for the model of ref [10]. The perturbative estimate for the contribution to S from techniquarks equals $1/2\pi$. The ellipse is the 90% confidence level contour for the global fit to the electroweak precision data with U kept at 0. The contour is for the reference Higgs mass of $m_H = 150$ GeV. Right Panel: Here the plot is obtained with a larger value of the hypercharge choice, according to which one of the two fermions is doubly charged and the other is singly charged under the electromagnetic interactions.

electroweak symmetry breaking [45–48]. This may happen due to the fact that the top quark is very heavy and hence strongly coupled to the electroweak symmetry breaking sector. Unfortunately the top-quark condensation mechanism per se seems to yield a too large top mass [49]. This problem can be addressed by re-introducing a technicolor theory [27]. One has also to invent a new strongly interacting theory coupling to the third generation of quarks and an additional strongly coupled $U(1)$ forbidding the formation of the bottom condensate. In this model one predicts the existence of topgluons, i.e. a massive color octet of vectors coupling mostly to the third generation. Due to the presence of the $U(1)$ interaction one predicts also the presence of a topcolor Z' particle.

Another promising idea is the top-seesaw model [6,50] in which the electroweak symmetry is broken thanks to the topcolor dynamics augmented with a seesaw mechanism involving an extra vectorlike quark, χ. The Higgs boson is composite, resulting from a $I = 1/2$ condensate of a left-handed top quark and a right-handed state of the new isosinglet quark. With the condensate mass scale at ~ 600 GeV, the vev of the Higgs field is at the right scale for electroweak symmetry breaking (EWSB) and the correct physical top mass will derive from the diagonalization of the mass matrix.

A summary of direct experimental limits on the existence of technicolor particles, as well as other resonances predicted in dynamical electroweak breaking scenarios can be found in [3, 51].

Most of the searches for technicolor resonances, have been performed in the context of a "multi-scale" technicolor model [36,37] in which "walking" of α_{TC} is achieved by the presence of a large number of technifermions, which are copies of the fundamental representation of the technicolor gauge group, or which belong to a few higher representations, or both. It is then expected, in a "technicolor straw man model"(TCSM) [52–54], that the low energy phenomenology will be determined by the lowest-lying bound states associated to the lightest technifermion family doublet. The lowest technicolor scale could be of a few hundred GeV's, and therefore these bound states, the isovector technipions $\pi_T^{\pm,0}$ and technirho $\rho^{\pm,0}$ and the isoscalar π'_T and techniomega ω_T, would have a good chance of being seen at the Tevatron and should certainly be accessible at the LHC. A limited number of parameters is assumed in the TCSM model: (i) N_{TC}, the number of technicolors of the $SU(N_{TC})$ group, (ii) N_D, the number of technifermion families (iii) χ, the mixing angle between the longitudinal vector bosons and the physical technipions, (iv) $Q = Q_U + Q_D$, the sum of the electric charges of the technifermions, (v) $m_V \sim m_A$, the mass parameters that control the strength of the technivector decay to a technipion and a transversely polarized electroweak boson (e.g., $\omega_T \to \pi_T^0 + \gamma$), (vi) $|\epsilon_{\rho\omega}|$, a mixing amplitude between ρ_T^0 and ω_T, and (vii) $m_{\rho_T}, m_{\omega_T}, m_{\pi_T}$, the masses of the vector resonances and of the technipions.

At LEP, in technicolor searches based on the TCSM [55–58] the processes considered were: $e^+e^- \to \rho_T^0, \omega_T \to \pi_T^+\pi_T^- \to b\bar{q}\bar{b}q'$, as well as final states $\pi_T^0\gamma \to b\bar{b}\gamma$ and $W\pi_T$. As a result of

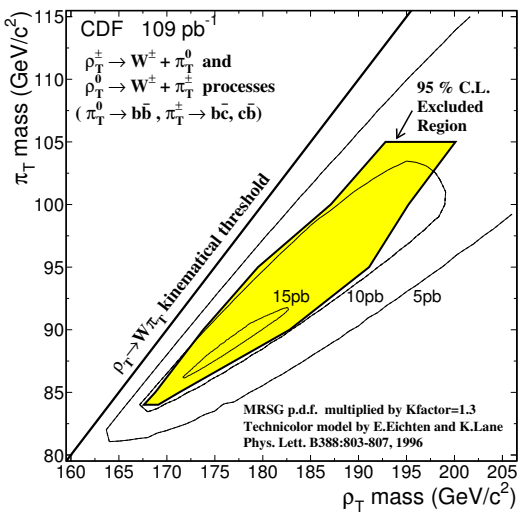

Fig. 12.3: Cross section contours, and 95% exclusion region in the $m(\pi_T), m(\rho_T)$ plane, from the lepton + 2 jets signal (from ref. [66]).

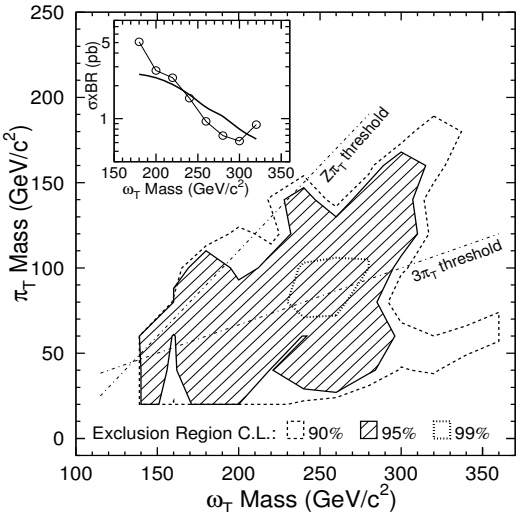

Fig. 12.4: Mass region excluded by the search for a light techniomega decaying to a technipion and a photon, with π_T decaying to two jets, with one tagged b -jet. (Inset: cross section limit for m_{π_T} = 120 GeV) [67]

these searches, an excluded region was obtained in the $(M_{\pi_T}, m_{\rho_T/\omega_T})$ plane. An upper bound of 87 GeV is obtained on the mass of π_T, at 95% CL, in the TCSM with $N_D = 9,\ (\chi = 1/3)$, independent of the mass of the vector states m_{ρ_T}, m_{ω_T}. This limit is somewhat reduced for larger values of the angle χ.

Presently, the most stringent experimental constraints on masses of technicolor particles are derived from Tevatron searches. Since technipions, similarly to the Higgs, are expected to couple preferentially to the heavier fermions, one possible signal of technicolor would be the detection of leptoquarks (color-triplet technipion) of the second or third generation, decaying to $b\tau, c\nu$ or $b\nu$. Pair production of these leptoquarks should be enhanced by the s-channel exchange of the color octet technirho resonance, $\rho_8 \to 2\pi_{LQ}$, coupling in a vector dominance model (VDM) to the gluon propagator. Searches for these processes [59, 60] have excluded regions of the $m_{\pi_{LQ}} - m_{\rho_T}$ plane, in the kinematically allowed areas of phase space. Typically, the limit on m_{ρ_T} is about 600 GeV (for $m_{\pi_T} < m_t$ in the $c\bar{c}\nu\bar{\nu}$ channel), but depends on the assumed value of the mass difference $\Delta M = m_{\pi_8} - m_{\pi_{LQ}}$. For high masses of technipions, a color-octet technirho could decay to di-jets. The mass range $350 < m_{\rho_8} < 440$ GeV, has been excluded [61, 62] in the $\rho_8 \to b\bar{b}$ channel. The absence of such $b\bar{b}$ mass peak also serves to set limits, depending on the assumed width of the resonance, on the masses of topgluon states. The above limits on the color octet vector resonance carry high uncertainty as it has been shown that the coupling of the state to two gluons is forbidden by gauge invariance [63] in a VDM, although higher order operators will lead to such couplings [64]. Furthermore, it has been argued [65] that in a model deviating even slightly from VDM, where some direct coupling exists between a quark and the interaction eigenstate of a technihadron, the coupling of the quark to the physical technirho would be highly suppressed.

Searches at the Tevatron have also been performed in the context of the TCSM model described above. The principal decay channels of ρ_T are $\pi_T\pi_T$, $V\pi_T$ and VV, $(V = W$ or $Z)$, but depending on the mass relations, branching ratios vary or some decay channels could be closed. Searches for event topologies containing leptons + jets [66, 68], or 4-jets were therefore performed, with selection of b-jets in the final state to reduce the backgrounds. The resulting contours of exclusion are shown in Fig. 12.3. Even with b-tagging of the jets, large backgrounds from W + heavy flavor, mistags, $t\bar{t}$ and single top events remain. Similarly, in the absence of evidence for peaks in the $\{m(\gamma bj) - m(bj)\}$ distribution, searches [67, 68] for $\omega_T \to \gamma\pi_T$ followed by $\pi_T \to b\bar{b}$ have also led to cross section limits, or to

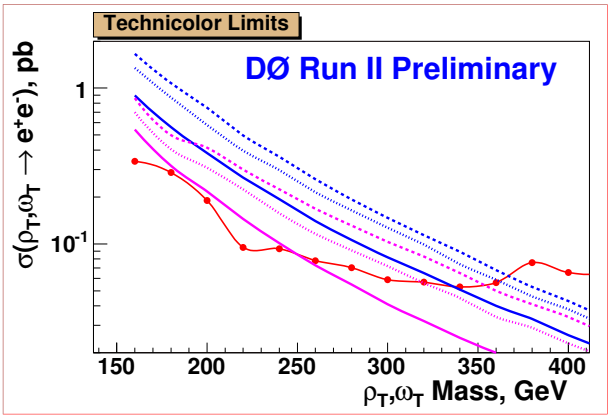

Fig. 12.5: Solid line with dots: 95% cross section upper bounds on ρ_T, ω_T cross section times branching ratio into ee. The various curves are predictions under certain assumptions of mass difference ($m(\rho_T) - m(\pi_T)$ = 60, 100 GeV) or of the parameter m_V = 500, 200 and 100 GeV (see ref. [70]).

exclusion regions of approximately $150 < m_{\omega_T} < 300$ GeV when $m_{\omega_T} > m_Z + m_{\pi_T}$ (see Fig. 12.4). Another relatively clean possible signature, which will be enhanced if decays of the vector resonances to technipions are kinematically closed, is a Z'-like peak in the di-lepton invariant mass: $\rho_T, \omega_T \rightarrow e^+e^-$. Fig. 12.5 shows preliminary bounds from D0 [69, 70] on the cross section times branching ratio of this process, obtained in RunII.

At the LHC, fast simulation studies [71], performed in the context of an earlier version of the TCSM model, implemented in PYTHIA, suggest that the technirho, techniomega and technipions could be detected up to masses of around 1 TeV. The LHC reach depends strongly on the assumed parameters, as the various branching ratios and decay widths are sensitive to the relative masses, as well as the mixing angles. Nevertheless, depending on parameters, a variety of signals can be investigated. For example, with an integrated luminosity of 30 fb^{-1}, the technirho can be observed up to masses of $\sim$ 800 GeV and the technipion up to $\sim$ 500 GeV, in channels: $\rho_T^{\pm} \rightarrow W^{\pm}Z$, $\rho_T^{\pm} \rightarrow \pi_T^{\pm}Z$ and $\rho_T^{\pm} \rightarrow W^{\pm}\pi_T^0$, when the vector bosons decay leptonically and the technipions decay to heavy flavor quarks. Fig. 12.6 shows an example of some specific cases of ρ_T resonances. It has been assumed that the π_T coupling to the top is small, as one would expect in topcolor models. As emphasized above, such plots are meant to be only indicative of the expected signals as the results are parameter dependent and as the branching ratios do not account for certain possible decays [53], implemented in later version of PYTHIA. The production of $\rho_T^{\pm}$ by a vector boson fusion process is another possibility [72], which could complement the $q\bar{q}$ fusion process. In all cases, it will be important to have efficient $b-$tagging of jets, and good lepton-jet discrimination.

At the ILC, a big advantage is the clean final state which allows reconstruction of hadronic decay modes of the W's, although di-jets will tend to have small opening angle because of the kinematic boost. Depending on the center of mass energy, resonances could be observed up to $\sim$ 2 TeV in channels of resonant vector boson scattering or of vector boson fusion producing fermion pairs, including top pairs. A summary of the potential for observing scalar and vector resonances at the ILC can be found, for example in [73–75]. In [74], expected bounds on the BESS model [76, 77] parameters are shown. This model assumes a triplet of vector resonances $V^{\pm,0}$ with parameters describing the mixing to the electroweak gauge bosons and the coupling to the fermions (see Section 11).

The topcolor models mentioned above have a rich phenomenology (for a review, see [3]). A triplet of top pions of mass $\sim$ 200 GeV could look like W' or Z' decaying to the third generation, and a scalar top Higgs could decay by the flavor changing process $\pi_t^{0'} \rightarrow \bar{t}c$. Color octet topgluons will produce resonances in the $t\bar{t}$ system. In the top condensation see-saw model, in general several composite scalars are predicted [6, 7]. From a phenomenological point of view, the mass of the isosinglet quark may be

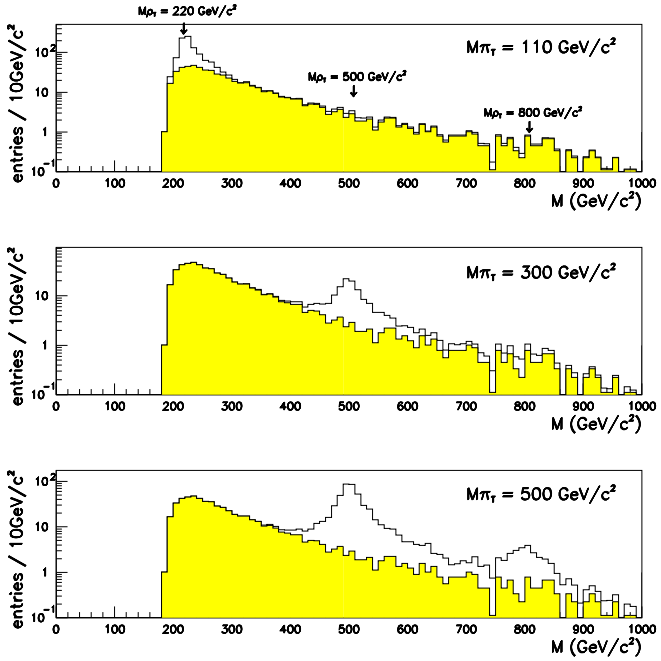

Fig. 12.6: $\rho_T^{\pm} \to W^{\pm}Z$: expected signals and background at the LHC, for 30 fb^{-1} and for different masses of the techni-resonances (from ref. [71]).

too high ($\sim$ 4 TeV) to be easily observed at the LHC, but a heavy Higgs ($m_H \sim$ TeV) is predicted and the mixing between the interaction states of t and of χ of same chirality affects the interaction of the physical top with the gauge bosons [41].

Other promising signatures for technicolor have been recently suggested. One very interesting possibility is the discovery of a fourth family of leptons, which could serve to confirm the model, discussed above, of electroweak symmetry breaking from technifermions in higher dimensional representations of the technicolor gauge group [10]. In this theory one would also expect a light composite Higgs, and the associated production of this Higgs boson with vector gauge bosons could be enhanced with respect to the Standard Model [78] (see Section 12.5). Another striking signal [79] (see also Section 12.6) would be a strong narrow resonance in the $\tau\tau$ and $\gamma\gamma$ channels. Indeed, a light technipion could be abundantly produced by gg fusion via techniquark loops, or by $b\bar{b}$ annihilation. The large enhancement factors predicted in models of dynamical symmetry breaking for resonances in these channels will allow to distinguish these technipions from the light scalars of the Standard Model or of Supersymmetry.

Many other phenomena possibly observed at the LHC could be interpreted in the context of a technicolor model, and indeed, it is by combining different signatures that confusion with other models can be cleared and that the nature of these resonances could be understood. For example, pair production of leptoquarks could be enhanced by a technirho resonance, as discussed above; or a Z'-like signature could signal a technivector resonance decay into leptons; a narrow $t\bar{t}$ or $b\bar{b}$ resonance which is non-flavour-universal can also signal topgluons (or leptophobic Z'). It is intriguing that an excess (not statistically significant) of $t\bar{t}$ events with an invariant mass around $\sim$ 500 GeV at the Tevatron [80, 81], could be a hint for the existence of such a resonance.

12.2 Extended technicolor

Nick Evans

The idea of breaking electroweak symmetry by a dynamically generated fermion condensate is both elegant and phenomenologically achievable. The harder challenge for such technicolor theories is to feed the electroweak symmetry breaking order parameter down to generate the diverse masses of the standard model fermions. The top mass presents a particular challenge because its large mass cannot be considered a small perturbation on the electroweak scale.

The most appealing mechanism for generating the standard model fermion, f, masses is extended technicolor [18, 82]. The technicolor gauge group is unified at high energies with a gauged flavour symmetry of the standard model fermions. This symmetry is then broken above the technicolor scale leaving massive gauge bosons that link the standard model fermions to the technicolour sector. The basic fermion mass generation mechanism is depicted in figure (12.7). The resulting mass generated is given in terms of the techniquark condensate $\langle \bar{T}T \rangle$ by

$$m_f \simeq \frac{g_{ETC}^2}{M_{ETC}^2} \langle \bar{T}T \rangle \tag{12.2}$$

where g_{ETC} and M_{ETC} are the coupling and mass of the ETC gauge boson.

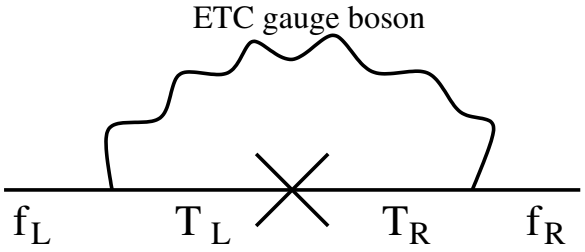

Fig. 12.7: ETC mass generation mechanism for a standard model fermion f. The ETC gauge boson converts f to a techni-fermion, T. The chirality mixing of the interactions is explicitly shown.

12.2.1 Model building

Many ETC models exist in the literature including [18, 19, 35, 82–91]. There are two common patterns chosen for the ETC gauge symmetry (see Fig 12.8). A natural choice is to gauge the family symmetry of the standard model fermions and then unify it with technicolor to give an SU(N+3) ETC group. Such a model will have a partner techni-fermion for each member of a standard model family - so called one family technicolor models. The ETC group is envisaged to be broken in the cascading pattern

$$SU(N+3) \rightarrow SU(N+2) \rightarrow SU(N+1) \rightarrow SU(N) \tag{12.3}$$

If the breakings occur at the scales of a few 100 TeV, a few 10TeV and of order a few TeV then the rough structure of the three family mass hierarchy is reproduced.

Another commonly used pattern of ETC leaves a one doublet technicolor model and appeals to the ideas of Pati Salam unification of quarks and leptons [92]. For example for the third family one might gauge the SU(4) flavour symmetry on the three colors of quarks and the tau lepton doublet. This could then be unified at high scales with the technicolor group leaving an SU(N+4) ETC group and a breaking pattern

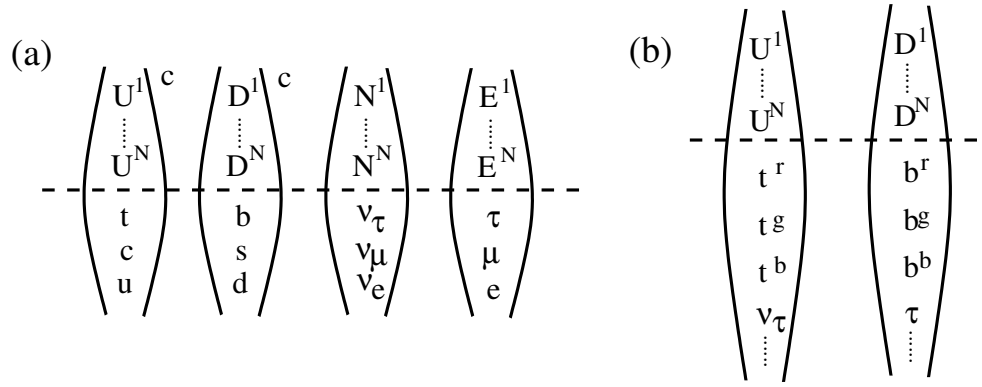

Fig. 12.8: Example ETC fermion multiplets - SU(N) technicolor acts on the techni-quarks with colors $1..N$ above the dashed line. The ETC group acts on the techni-quarks and standard model fermions so there are gauge bosons that convert one to the other. In (a) the four fermion multiplets of a one family model are shown and the ETC group is a family symmetry group. The c index indicates which mulitplets have QCD color. In (b) a one doublet model's multiplets are shown. Here the ETC group contains the QCD color symmetry acting on the r, g, b colors of quarks, and leptons are the "fourth" color.

$$SU(N+4) \rightarrow SU(N+3) \rightarrow SU(N) \otimes SU(3) \tag{12.4}$$

Expanding this scenario to incorporate the full set of standard model fermions involves promoting the ETC group to SU(N+12) and a very complicated symmetry breaking pattern.

Many examples of the ETC symmetry breaking mechanisms exist in the literature including entirely dynamical sectors or less satisfactorily higgs fields. Another idea that has been proposed is that the ETC group might sequentially break itself via a "tumbling" mechanism [93–96] in which non-color singlet condensates are formed by the ETC dynamics. All these models are typically complicated since they seek to explain many different symmetry breaking sectors. Given that we still struggle to understand electroweak symmetry breaking these mechanisms are perhaps best left for the future if technicolor is discovered.

The ETC schemes sketched so far contain no dynamics capable of explaining the splitting in masses between different weak isospin partner fermions. The most marked splitting is in the top bottom quark doublet which must have the lowest ETC scale - such isospin breaking will be apparent in any initial discovery of such a sector.

One solution is to make the ETC gauge symmetries chiral (eg [87–89]) so that the right handed top and bottom quarks transform under different groups with potentially different breaking scales and couplings. The ETC symmetry breaking sector must then be further complicated as these different ETC groups are broken together to leave a single technicolor group. Extra fermions must be included in such a model to maintain the anomaly freedom of the ETC gauge groups and a mechanism must be found to give these fermions masses above current limits. Such models predict a rich structure of new physics beyond the standard model.

Alternatively the right handed top or bottom could be placed in a different representation of a single ETC group (eg [42]). This approach is a model building challenge since the top and bottom must emerge without extra fields present at low energy from the higher dimensional representation.

The generation of the fermion CKM mixing angles and CP violation are also a challenge to ETC models [97–99]. Models have been made in which these aspects of the mass spectrum are inherited from physics at higher energy scales without explanation [88, 89]. There are models that more directly attack their generation which typically try to arrange the mixings' emergence from a dynamical vacuum

alignment problem (eg [99]). The small size of the neutrino masses need explanation too. Recently dynamical generation of a Majorana mass for the right handed neutrinos has been investigated leading to a see-saw mechanism to suppress their masses [19].

Finally we note that in the schemes discussed above the SU(2) gauge symmetry of the weak interactions was assumed to commute with the ETC group. In principle this need not be the case. One could imagine a chiral ETC symmetry as large as

$$SU(N+24)_R \otimes SU(N+24)_L \tag{12.5}$$

with the weak SU(2) embedded in the ETC dynamics. Such models are called non-commuting ETC [25, 100].

12.2.2 Indirect constraints

A number of indirect constraints exist on ETC theories.

12.2.2.1 Flavour changing neutral currents

The gauging of flavour symmetries is well known to induce flavour changing neutral currents (FCNC) since the flavour group's gauge eigenstates cannot be expected to match the standard model fermion mass eigenstates. The absence of FCNC in the standard model makes these constraints (from kaon and D-meson physics), on the first two families, very restrictive [18, 101]. In fact such a flavour gauge boson must have a mass in excess of 500 TeV. This is hard to reconcile in an ETC model with the measured values of the second family quark masses.

An early model building suggestion for overcoming the difficulty was walking technicolor [20,22]. If the technicolor gauge coupling runs close to an infra-red fixed point, so it is strong over a large energy range, then the techni-fermion condensate is enhanced pushing up the ETC scale needed to generate a particular fermion mass. Pushing the ETC scale up by an order of magnitude does though require walking dynamics over a long energy regime.

An alternative solution has been to build models that have a GIM mechanism [88, 89, 102] in the spirit of the standard model. These models have separate ETC groups acting on the left handed doublets, and on both the $+1/2$ and $-1/2$ isospin right handed doublets. The constraints on such models from FCNC are very much weaker than on normal ETC models.

12.2.2.2 ρ/T parameter

To generate the large top mass by a standard ETC mechanism requires the ETC scale to be as low as 1 TeV. Since this dynamics breaks isospin in order to explain the top bottom mass splitting, the light ETC gauge bosons must also violate isospin. These gauge bosons will enter into virtual contributions to the W and Z boson masses through diagrams like those in Fig 12.9(a). There will thus be contributions to the $\delta\rho$ or T parameter of rough order of magnitude

$$\alpha T \sim \frac{v^2}{M_{ETC}^2} \tag{12.6}$$

where α is the electromagnetic coupling.

For a 1TeV ETC scale such contributions are huge ($T \sim 10$!) [103, 104]. One concludes the ETC scale must be larger than about 4TeV to stand a chance of being compatible with precision data. Some method for enhancing the top mass over the predictions from naive ETC are then needed.

The ETC isospin breaking will also generate techni-fermion masses which break isospin. Typically one might expect this mass splitting, ΔM, to be of order the top bottom mass splitting. The contribution to T is given by roughly [5]

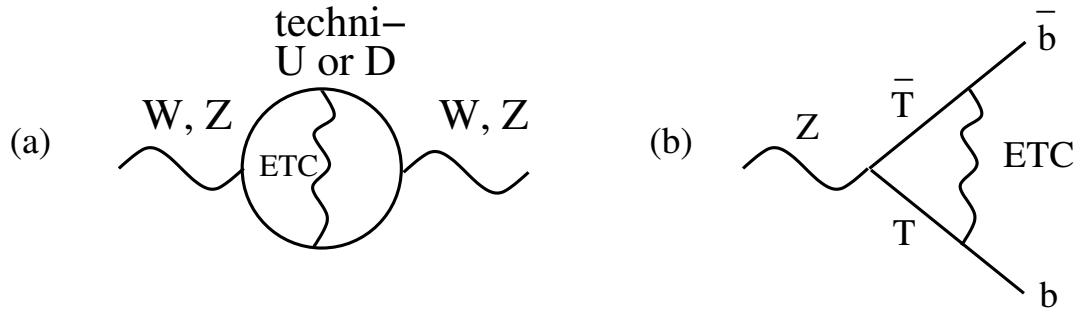

Fig. 12.9: (a) Isospin violating ETC gauge bosons contribute to the mass of the W and Z bosons through their couplings within loops of techni-fermions. The contributions to the T parameter can be very large. (b) ETC gauge bosons that couple the left handed bottom quark to the techni-quark sector generate substantial corrections to the $Zb\bar{b}$ vertex.

$$T \sim \frac{N_{TC}}{12\pi^2\alpha}\frac{\Delta M^2}{v^2} \sim 0.6 N_{TC}\frac{\Delta M^2}{m_t^2} \tag{12.7}$$

with N_{TC} the number of techni-colors, which lies close to the upper experimental bound.

12.2.2.3 $Zb\bar{b}$ vertex

The most strongly coupled ETC gauge bosons responsible for the top mass must also couple to the left handed bottom quark. The exchange of such a gauge boson across the $Zb\bar{b}$ vertex, as shown in Fig 12.9(b), leads to a correction to the $Zb\bar{b}$ width that has been estimated to be of the order [105]

$$\frac{\delta\Gamma}{\Gamma} \sim -6.5\% \left(\frac{m_t}{175GeV}\right) \tag{12.8}$$

Such a large contribution is not compatible with data. If a mechanism for enhancing the top mass over naive ETC estimates can be found then this contribution will fall off quadratically as the ETC scale is raised. Finally we note that positive corrections to the width are possible in non-commuting technicolor theories [25].

12.2.3 Strong ETC and top condensation

It is clear from the estimates of the T parameter and the corrections to the $Zb\bar{b}$ vertex that a naive ETC model can not generate the observed top mass. The lowest ETC scale must be pushed up to of order 4 TeV or above. One mechanism for enhancing the top mass is walking technicolor which enhances the techni-fermion condensate. In such a scenario the ETC interactions will themselves be strong [106–108] and there will be further non-perturbative enhancement of the top mass. The extreme version of such a model has the ETC interactions on the top quark sufficiently large on their own that they generate a top quark condensate and the top mass independently of the rest of the ETC sector [27, 45, 46, 49]. When the ETC couplings lie close to the critical values for triggering chiral symmetry breaking on their own, small isospin violating effects, such as from an extra U(1) gauge group, which tip the combined coupling super critical may generate large top bottom splitting. This would reduce tension with the T parameter measurements. If strong ETC is the route nature has chosen it is most likely that a combination of all these ideas are responsible for the large top mass.

12.2.4 Direct searches for ETC

ETC gauge bosons are flavour gauge bosons and their presence can be seen as an enhancement of a number of standard model processes [109]. They most strongly couple to the third family where they are most likely to be observed first. Models with additional gauged flavour symmetries on the quarks such as top color models [27] will generate enhanced dijet production in hadronic machines. ETC gauge bosons coupling to quarks may also mediate large enhancement of single top production processes over the standard model rate. A wider set of models was considered in [110,111] which also include couplings to leptons - the ETC gauge bosons then give new contributions in Drell Yan production.

12.3 Composite Higgs from higher representations

Dennis D. Dietrich

12.3.1 The minimal walking technicolour theory

Technicolour theories [1–4] can be constructed with techniquarks in higher dimensional representations [18, 36, 38] of the technicolour gauge group. One of these theories, denoted by S($N, N_{\rm f}$)=S(2,2), with two techniflavours in the two-index symmetric representation of SU(2) [1] [10, 40, 112, 113] is found to be in agreement with electroweak precision data [39]. This variant of the model is closest to the currently available data and is the main subject of this contribution. There exists another version, S(3,2), which is consistent at the two sigma (standard deviation) level and which is discussed briefly toward the end of this contribution.

The important feature of the S(2,2) theory is that, with the smallest possible number of techniflavours and -colours, it is quasi conformal [8, 9], that is it possesses a walking coupling constant (see Introduction, Fig. 12.1). The small number of additional degrees of freedom leads only to small corrections to the standard model at energies below $\Lambda_{\rm TC}$. The quasi-conformality allows to generate the required masses for the ordinary fermions by means of extended technicolour interactions (ETC) [42, 43, 91, 114] while avoiding flavour-changing neutral currents and lepton number violation, which would be at odds with data [35] (see below).

Furthermore, the walking of a theory has the capability to reduce the mass of the composite scalar (the Higgs) below the value of the typical scale of the underlying theory. Due to its very near conformality, the theory S(2,2) is likely to feature a remarkably light Higgs (see below). Whether a technicolour theory is nearly conformal depends on the number of technicolours and techniflavours as well as of the representation of the techniquarks. If a theory is not conformal for a given number of techniflavours it will enter the conformal phase when their number is increased. At leading order, the point where this happens can be characterised by the anomalous dimension of the quark mass operator becoming unity [114, 115] [2]. Hence, for a given number of technicolours and a given representation of the technicolour gauge group, the aforementioned criterion defines the critical number of techniflavours. Based on the two-loop beta-function, which in the t'Hooft scheme is exact, the critical number of flavours for a theory with adjoint techniquarks is found to be $N_{\rm f,crit.} = 2.075$, independent of the number of technicolours. The squared mass of the Higgs scalar is suppressed with respect to the scale of the theory by a factor of the small difference of the critical number of flavours and the actual number of flavours, $(N_{\rm f,crit.} - N_{\rm f})$ [10, 40], [3] the latter of which is necessarily an even integer. This leads to an estimated mass for the composite Higgs of about 150 GeV [10, 40].

[1] For two (techni-)colours the two-index symmetric representation coincides with the adjoint representation.

[2] At any finite higher order the criterion will usually receive corrections.

[3] Note, however, that this result might acquire corrections [29, 116]. Near the conformal phase transition other states could become light, which, in turn, could affect the argument supporting universal behavior near the phase transition [117]. That, however, need not change the result. Especially, a vanishing chiral symmetry scale does not imply that the chiral partner of the pions does not become parametrically lighter and narrow near the phase transition, as the self coupling of the scalar is also expected to vanish near a continuous phase transition [35].

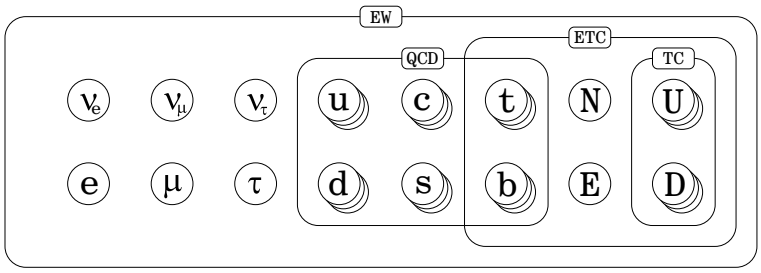

q	(I)	(II)	(III)
U	$+2/3$	$+1/2$	$+1$
D	$-1/3$	$-1/2$	0
N	0	$+1/2$	-1
E	-1	$-1/2$	-2

Fig. 12.10: Matter content of the S(2,2) model: *Left panel:* Staggered circles represent the number of colour degrees of freedom of a particle. Boxes denote under which subset of the gauge group the particles transform. Usually ETC models comprise all massive particles. Here, however, the matter content of the residual ETC model of Ref. [35] is indicated. *Right panel:* Electric charges, q, of the new particles—U (techniup), D (technidown), as well as N and E (fourth family leptons)—in the three studied cases.

In the S(2,2) model the topological Witten anomaly [118] is evaded by including a fourth lepton family [10, 40]. The matter content of the model is summarised in the left panel of Fig. 12.10. At this point, only the hypercharge assignment of the new particles remains to be specified. It is constrained but not uniquely determined by requiring the absence of gauge anomalies [10, 40]. Here three possibilities for the electric charge, q, of the techniup (U), technidown (D), the fourth neutrino (N), and the fourth electron (E) are considered (see Fig. 12.10, right panel).

In case (I) the neutrino, N, can constitute a non-hadronic component of dark matter. The technicolour of any number of techniquarks in the adjoint representation can be neutralised by adding technigluons. With respect to the standard model sector, such bound states interact only weakly and behave like leptons. In case (III) a D techniquark whose colour has been neutralised by additional gluons can contribute to dark matter. In the same case, (III), bound states of two D techniquarks and in case (II) UD bound states represent potential technihadronic contributions to dark matter. For more details on these technihadrons and dark matter candidates see Section 12.4.

In [10, 40, 112, 113] predictions from these models have been compared to electroweak precision data. To this end the oblique parameters S and T [119] have been calculated and compared to data. They quantify the contribution to the vacuum polarisation of the gauge bosons from the particles which are not contained in the standard model. Therefore, per definition, the standard model with a reference Higgs mass has $S = 0 = T$. S is a measure for the mixing between the photon and the Z_0, while T measures the additional breaking of the custodial symmetry. In Fig. 12.2 of the Introduction, the areas filled in black depict the perturbatively calculated values taken by the oblique parameters for degenerate techniquarks and when the masses of the two additional leptons are varied independently between one and ten m_Z. The ellipse represents the 68% confidence level contour from the global fit to data in [39]. There it is assumed that the third oblique parameter, U, is zero, which is consistent with the values predicted in the present framework. In the fractionally charged case there is no variation in the direction of S and varying the masses of the leptons gives a vertical line exactly in the opening of the area shaded in black.

Already this perturbative analysis of the oblique parameters, which can be seen as conservative, displays a sizeable overlap with the range favoured by the data. In quasi-conformal theories like the present one, the techniquarks' contribution to S is lowered by non-perturbative effects [32–34, 120, 121], corresponding to a reduction of about 20% [34, 121]. The aforementioned reduction of the value of S caused by the walking of the coupling has also been confirmed by a holographic analysis of technicolour theories [122]. If the reduction of 20% is taken into account the overlap between the 68% level of confidence ellipse and the values predicted for the S(2,2) technicolour model becomes even larger (see Fig. 12.11). Especially, an overlap with the right branch of the area filled in black can be achieved.

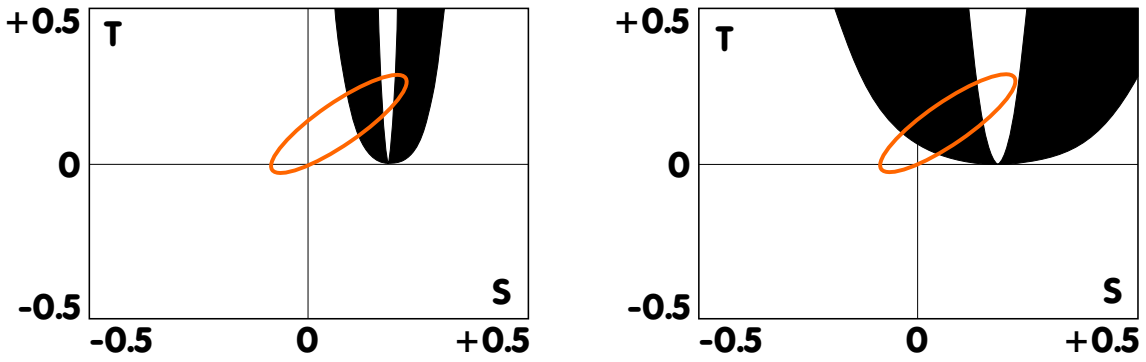

(a) Standard-model-like charge assignment (I)

(b) Integerly charged leptons (III)

Fig. 12.11: Including nonperturbative corrections. The black area represents the accessible range for the oblique parameters S and T for the masses of the fourth family leptons $m_E, m_N \in [m_Z; 10m_Z]$ and with degenerate techniquarks, which corresponds to a contribution of $0.8/2\pi$ to S from the latter. The ellipse is the 68% confidence level contour for a global fit to electroweak precision data [39] with the third oblique parameter U put to zero and for a Higgs mass of $m_H = 150$ GeV, as expected for the S(2,2) model. Putting U to zero is also consistent with the S(2,2) model, where it lies typically between 0 and 0.05.

In the purely perturbative computation of the oblique parameters, the overlap between the ellipses and the black shaded areas in Fig. 12.2 of the Introduction corresponds to the masses depicted in Fig. 12.12 of the present contribution. In the cases (I) and (III) the main feature is a mass gap of the order of m_Z between the new leptons by which N is lighter (m_2) than E (m_1). The mass gap is mostly determined by the limits in $(S - T)$-direction. In the case (II) an additional branch with the opposite sign for the mass gap is present. Including nonperturbative corrections to the technicolour sector, the additional overlap of the 68% level of confidence contour with the right-hand side of the black areas in Fig. 12.11 translates to a second branch also for cases (I) and (III), which is otherwise suppressed by the limit on S. In the present model the expected mass for the composite Higgs is 150 GeV, but even if it was as heavy as 1 TeV there would still be an overlap to the data at the 68% level of confidence.

Recently, there have been indications that the experimental constraints on the oblique parameters are much weaker than obtained in previous analyses [123,124]. In [123] it has been demonstrated that the bounds become much less stringent when the uncertainty in the triple and quartic gauge boson couplings is taken into account. Hence, the range of favoured masses tends to be even larger.

12.3.2 Extended technicolour

As mentioned above, the masses of the standard model fermions are to be generated by ETC interactions, that is the direct exchange of ETC gauge bosons between the fermions of the standard model and the techniquarks. For this purpose the TC model is embedded in a larger gauge group, whose additional symmetries are broken successively. In the broken phase of the ETC group typically three types of effective four-fermion interactions occur, (a) $\bar{Q}Q\bar{Q}Q\Lambda_{\rm ETC}^{-2}$, (b) $\bar{\psi}\psi\bar{Q}Q\Lambda_{\rm ETC}^{-2}$, and (c) $\bar{\psi}\psi\bar{\psi}\psi\Lambda_{\rm ETC}^{-2}$, where Q stands for any techniquark and ψ represents any standard model fermion. (Different fermion types may be coupled together in this way.) In the broken phase of the TC group a chiral condensate of techniquarks develops, $\bar{Q}Q \to \langle\bar{Q}Q\rangle$, which leads to the following contributions: (a) $\bar{Q}Q\langle\bar{Q}Q\rangle\Lambda_{\rm ETC}^{-2}$, (b) $\bar{\psi}\psi\langle\bar{Q}Q\rangle\Lambda_{\rm ETC}^{-2}$, and (c) $\bar{\psi}\psi\bar{\psi}\psi\Lambda_{\rm ETC}^{-2}$. Terms of the type (c) are a byproduct of the ETC mechanism and lead to flavour changing neutral currents and lepton number violation. If no suitable GIM mechanism [88, 89, 125, 126] can be devised, the breaking scale $\Lambda_{\rm ETC}$ must be sufficiently large to suppress these terms. Terms of the type (b) provide the masses for the standard model fermions. With a running

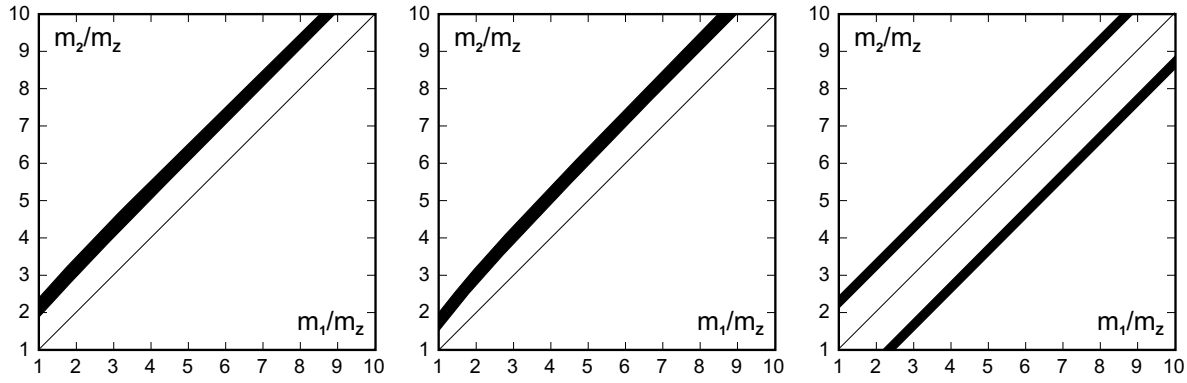

(a) Standard-model-like (I) (b) Integer charges (III) (c) Fractional charges (II)

Fig. 12.12: The black slabs mark the combination of masses favoured by electroweak precision data [39, 40] at the 68% level of confidence based on the conservative perturbative estimate. m_1 (m_2) denotes the mass of the fourth family lepton with the higher (lower) charge. The black stripes do not correspond exactly to the overlap of the parabolic area with the 68% ellipse in Fig. 12.2 of the Introduction but with a polygonal area defined by $-0.1 < S + T < +0.5$, $-0.15 < S - T < +0.025$, and $S < 0.22$.

TC sector (see Introduction, Fig. 12.1, left panel) the one-loop estimate for the mass, $m_{\rm t}$, is given by [35]

$$m_{\rm t} = \frac{N}{4\pi^2}\frac{\Sigma(0)^2}{\Lambda_{ETC}^2}\Sigma(0), \tag{12.9}$$

where $\Sigma(0)$ stands for the self energy of the techniquark at zero momentum and is of the order of 1 TeV. In a walking TC theory, where the scale $\Lambda_{\rm ETC}$ can be larger than $\Sigma(0)$ (see Introduction, Fig. 12.1, right panel), the attainable mass, $m_{\rm t}$, is enhanced by a factor of up to $\Lambda_{\rm ETC}/\Sigma(0)$ [19, 35],

$$m_{\rm t} = \frac{N}{4\pi^2}\frac{\Sigma(0)}{\Lambda_{ETC}}\Sigma(0). \tag{12.10}$$

Therefore, the top quark mass can still be generated if $\Lambda_{\rm ETC}$ = 4-8 TeV [35], whereas, in the running case, it is already difficult to reach it with $\Lambda_{\rm ETC}$ = 1 TeV. Thus, $\Lambda_{\rm ETC}$ may be sufficiently large to suppress terms of type (c). Terms of type (a) are even more enhanced than terms of type (b) and provide very large masses for additional (pseudo) Goldstone bosons, which do not become the longitudinal degrees of freedom of the gauge bosons and which might be present depending on the symmetry breaking pattern. Thereby their direct detection is impeded.

After these general considerations we consider below a concrete ETC model [35], which generates the mass of the top quark. It contains the type (I) S(2,2) model. The matter fields are arranged in a SU(7) multiplet and a SU(4) right-handed part [35],

$$\mathrm{SU}(7) : \left\{ \left[\begin{pmatrix} U^a \\ D^a \end{pmatrix}_L , \begin{pmatrix} N \\ E \end{pmatrix}_L , \begin{pmatrix} t^c \\ b^c \end{pmatrix}_L \right] , [U_R^a\ ,\ N_R\ ,\ t_R^c] \right\} \quad \times \quad \mathrm{SU}(4) : \{[D_R^a\ , E_R]\}. \tag{12.11}$$

a and c are the proto TC and QCD indices, respectively. The symmetry breaking pattern is

$$\mathrm{SU}(7) \times \mathrm{SU}(4) \times \mathrm{SU}(3) \rightarrow \mathrm{SO}(3)_{\rm TC} \times \mathrm{SU}(3)_{\rm QCD}, \tag{12.12}$$

which exploits the fact that the fundamental representation of SO(3) coincides with the adjoint of SU(2). Here the bottom quark is excluded from the second multiplet because its mass is negligible compared to the top mass. It will be generated by the breaking of a larger ETC group at higher energies, which will certainly lie outside the reach of experiments of the near future. The specific arrangement of the particles implies that, if the top mass is generated, the mass gap between U and D as well as between

N and E must be of the same order. This is consistent with the size of the mass gap favored by data presented in reference [39]. Especially, in view of the findings of [123] the above scheme represents a viable candidate for a residual ETC model. The same conclusion is obtained from direct calculation of the oblique parameters in [35].

12.3.3 A different variant, S(3,2)

The S(2,2) model with two technicolours and two techniflavours in the two-index symmetric representation represents the scenario favoured by data. The runner-up is the S(3,2) model (three technicolours, two techniflavours). Its perturbative contribution to the S parameter equals $1/\pi$, which is exactly twice the value of the S(2,2) model. Thereby, according to [39], S(3,2) lies still within two standard deviations from the mean value even before taking into account non-perturbative reductions. The set-up S(3,2) is not as close to the conformal window as S(2,2), whence a heavier Higgs with $m_H = 170 - 300$ GeV [10] is expected. The symmetric representation of SU(3) is of dimension six. Hence, from the point of view of the electroweak sector, the family of techniquarks comes in an even number of (colour-)copies, which does not trigger a topological Witten anomaly even without a fourth family of leptons. It does not feature the enhanced flavour symmetry SU($2N_f$) of the adjoint S(2,2), whence the breaking of S(3,2) only leads to the three Goldstone bosons, which represent the longitudinal degrees of freedom of the electroweak gauge bosons. In the case of S(2,2) one has a total of nine, that is six unabsorbed Goldstone bosons [127], because of the enhanced symmetry [SU($2N_f$=4)] for the adjoint matter (for more details see again Section 12.4). Hence, for energies below the technicolour scale $\Lambda_{\rm TC}$, which might be larger than 1 TeV, S(3,2) looks identical to the standard model; apart from a higher but not inconsistent contribution to the S parameter.

12.4 Minimal walking technicolor: effective theories and dark matter

Sven Bjarke Gudnason and Chris Kouvaris

In this contribution we examine the phenomenological implications of the technicolor theory with two techniquarks transforming according to the adjoint representation of $SU(2)$ [127] (see Section 12.3). The theory predicts Goldstone bosons that carry nonzero technibaryon number. These technibaryons must acquire a mass from some, yet unspecified, theory at a higher scale. Since we assume a bottom up approach we postpone the problem of producing the underlying theory providing these masses, but we expect it to be similar to the ETC type theory proposed in [35] (see Sections 12.2 and 12.3). If the technibaryon number is left intact by the ETC interactions, the lightest technibaryon (LTB) is stable and the hypercharge assignment can be chosen in a way that the LTB is also electrically neutral. The mass of the LTB is expected to be of the order of the electroweak scale. Therefore it has many features required for a dark matter component.

In the first part of the contribution, we provide the associated linear and non-linear effective theories. In the second part of this contribution we consider the scenario of one of the Goldstone bosons to be a dark matter component. We assume one of the Goldstone bosons to be neutral and we calculate its contribution to the dark matter density.

12.4.1 The model

The new dynamical sector underlying the Higgs mechanism we consider is an $SU(2)$ technicolor gauge group with two adjoint technifermions. The theory is asymptotically free if the number of flavors $N_f < 2.75$.

As it is shown in Ref. [8], the number of flavors $N_f = 2$ lies sufficiently close to the critical value for which an infrared stable fixed point emerges so the theory is a perfect candidate for a walking technicolor theory. Although the critical number of flavors is independent of the number of colors when

keeping the underlying fermions in the adjoint representation of the gauge group, the electroweak precision measurements do depend on it. Since the lowest number of colors is privileged by data [10, 40] we choose the two-technicolor theory.

Then the two adjoint fermions may be written as

$$T^a_L = \begin{pmatrix} U^a \\ D^a \end{pmatrix}_L , \qquad U^a_R , \quad D^a_R , \qquad a = 1, 2, 3 , \tag{12.13}$$

with a the adjoint technicolor index of $SU(2)$. The left fields are arranged in three doublets of the $SU(2)_L$ weak interactions in the standard fashion. The condensate is $\langle \bar{U}U + \bar{D}D \rangle$ which breaks spontaneously the electroweak symmetry.

Our additional matter content is essentially a copy of a standard model fermion family with quarks (here transforming in the adjoint of $SU(2)$) and the following lepton doublet in order to cancel Witten's global anomaly

$$\mathcal{L}_L = \begin{pmatrix} N \\ E \end{pmatrix}_L , \qquad N_R , \; E_R . \tag{12.14}$$

Since we do not wish to disturb the walking nature of the technicolor dynamics, the doublet (12.14) must be a technicolor singlet [10]. In general, the gauge anomalies cancel using the following generic hypercharge assignment

$$Y(T_L) = \frac{y}{2} , \qquad Y(U_R, D_R) = \left(\frac{y+1}{2}, \frac{y-1}{2} \right) , \tag{12.15}$$

$$Y(\mathcal{L}_L) = -3\frac{y}{2} , \qquad Y(N_R, E_R) = \left(\frac{-3y+1}{2}, \frac{-3y-1}{2} \right) , \tag{12.16}$$

where the parameter y can take any real value. In our notation the electric charge is $Q = T_3 + Y$, where T_3 is the weak isospin generator. One recovers the SM hypercharge assignment for $y = 1/3$. In [35], the SM hypercharge has been investigated in the context of an extended technicolor theory. Another interesting choice of the hypercharge is $y = 1$, which has been investigated, from the point of view of the electroweak precision measurements, in [10, 40]. In this case

$$Q(U) = 1 , \quad Q(D) = 0 , \quad Q(N) = -1 , \quad \text{and} \quad Q(E) = -2 , \quad \text{with} \quad y = 1 . \tag{12.17}$$

Notice that in this particular hypercharge assignment, the D technidown is electrically neutral.

Since we have two Dirac fermions in the adjoint representation of the gauge group, the global symmetry is $SU(4)$. To discuss the symmetry properties of the theory it is convenient to use the Weyl base for the fermions and arrange them in the following vector transforming according to the fundamental representation of $SU(4)$

$$Q = \begin{pmatrix} U_L \\ D_L \\ -i\sigma^2 U^*_R \\ -i\sigma^2 D^*_R \end{pmatrix} , \tag{12.18}$$

where U_L and D_L are the left handed techniup and technidown respectively and U_R and D_R are the corresponding right handed particles. Assuming the standard breaking to the maximal diagonal subgroup, the $SU(4)$ symmetry breaks spontaneously down to $SO(4)$. Such a breaking is driven by the following condensate

$$\langle Q^\alpha_i Q^\beta_j \epsilon_{\alpha\beta} E^{ij} \rangle = -2 \langle \overline{U}_R U_L + \overline{D}_R D_L \rangle , \tag{12.19}$$

where the indices $i, j = 1, \ldots, 4$ denote the components of the tetraplet of Q, and the Greek indices indicate the ordinary spin. The matrix E is a 4×4 matrix defined as $E = \sigma^1 \otimes \mathbb{1}$, where $\mathbb{1}$ is the

2-dimensional unit matrix. We have used $\epsilon_{\alpha\beta} = -i\sigma^2_{\alpha\beta}$ and $\langle U_L^\alpha {U_R}^{*\beta} \epsilon_{\alpha\beta}\rangle = -\langle \overline{U}_R U_L\rangle$. A similar expression holds for the D techniquark. The above condensate is invariant under an $SO(4)$ symmetry.

In terms of the underlying degrees of freedom, and focusing only on the techniflavor symmetries, there are nine Goldstone bosons, three of which, transforming like

$$\overline{D}_R U_L\,, \qquad \overline{U}_R D_L\,, \qquad \frac{1}{\sqrt{2}}(\overline{U}_R U_L - \overline{D}_R D_L)\,, \tag{12.20}$$

will be eaten by the longitudinal components of the massive electroweak gauge bosons. The electric charge is respectively one, minus one and zero. For the other six Goldstone bosons we have

$$U_L U_L,\quad D_L D_L,\quad U_L D_L\,, \qquad \text{with electric charges} \quad y+1,\ y-1,\ y\,, \tag{12.21}$$

together with the associated anti-particles. These Goldstone bosons (Eq. (12.21)) are di-technibaryons carrying technibaryon number. The technibaryon generator can be identified with one of the generators of $SU(4)$.

12.4.2 Effective theories

While the leptonic sector can be described within perturbation theory since it interacts only via electroweak interactions, the situation for the techniquarks is more involved since they combine into composite objects interacting strongly among themselves. It is therefore useful to construct low energy effective theories encoding the basic symmetry features of the underlying theory. We construct the linearly and nonlinearly realized low energy effective theories for our underlying theory. The theories we will present can be used to investigate relevant processes of interest at LHC and LC.

12.4.2.1 The linear realization

The relevant effective theory for the Higgs sector at the electroweak scale consists, in our model, of a light composite Higgs and nine Goldstone bosons. These can be assembled in the matrix

$$M = \left(\frac{\sigma}{2} + i\sqrt{2}\Pi^a\, X^a\right) E\,, \tag{12.22}$$

which transforms under the full $SU(4)$ group according to $M \to uMu^T$, with $u \in SU(4)$, and X^a are the generators of the $SU(4)$ group which do not leave invariant the vacuum expectation value $\langle M\rangle = vE/2$.

It is convenient to separate the fifteen generators of $SU(4)$ into the six that leave the vacuum invariant (S^a) and the other nine that do not (X^a). One can show that the S^a generators of the $SO(4)$ subgroup satisfy the following relation

$$S^a\, E + E\, S^{aT} = 0\,, \qquad \text{with} \qquad a = 1,\ldots,6\,. \tag{12.23}$$

The electroweak subgroup can be embedded in $SU(4)$, as explained in detail in [33]. The main difference here is that we have a more general definition of the hypercharge. The electroweak covariant derivative is

$$D_\mu M = \partial_\mu M - i\, g\left[G_\mu M + M G_\mu^T\right]\,, \tag{12.24}$$

with

$$G_\mu = \begin{pmatrix} W_\mu & 0 \\ 0 & -\frac{g'}{g}B_\mu^T \end{pmatrix} + \frac{y}{2}\frac{g'}{g}B_\mu \begin{pmatrix} 1 & 0 \\ 0 & -1 \end{pmatrix}\,, \quad W_\mu = W_\mu^a \frac{\tau^a}{2}\,, \quad B_\mu^T = B_\mu \frac{\tau^{3T}}{2} = B_\mu \frac{\tau^3}{2}\,, \tag{12.25}$$

where τ^a are the Pauli matrices. The generators satisfy the normalization conditions $\mathrm{Tr}[X^a\, X^b] = \delta^{ab}/2$, $\mathrm{Tr}[S^a\, S^b] = \delta^{ab}/2$ and $\mathrm{Tr}[SX] = 0$. Three of the Goldstone bosons in the unitary gauge, are absorbed in the longitudinal degrees of freedom of the massive weak gauge bosons while the extra six Goldstone bosons will acquire a mass due to extended technicolor interactions as well as the electroweak interactions per se. Assuming a bottom up approach we will introduce by hand a mass term for the Goldstone bosons. The new Higgs Lagrangian is then

$$\begin{aligned} L &= \frac{1}{2}\mathrm{Tr}\left[D_\mu M D^\mu M^\dagger\right] + \frac{m^2}{2}\mathrm{Tr}[MM^\dagger] \\ &- \frac{\lambda}{4}\mathrm{Tr}\left[MM^\dagger\right]^2 - \widetilde{\lambda}\mathrm{Tr}\left[MM^\dagger MM^\dagger\right] - \frac{1}{2}\,\Pi_a (M^2_{\mathrm{ETC}})^{ab}\Pi_b\,, \end{aligned} \tag{12.26}$$

with $m^2 > 0$ and a and b running over the six uneaten Goldstone bosons. The matrix M^2_{ETC} is dynamically generated and parametrizes our ignorance about the underlying extended technicolor model, yielding the specific mass texture. The pseudo Goldstone bosons are expected to acquire a mass of the order of a TeV. Direct and computable contributions from the electroweak corrections break $SU(4)$ explicitly down to $SU(2)_L \times SU(2)_R$ yielding an extra contribution to the uneaten Goldstone bosons. However the main contribution comes from the ETC interactions.

We stress that the expectation of a light composite Higgs relies on the assumption that the quantum chiral phase transition as function of number of flavors near the nontrivial infrared fixed point is smooth and possibly of second order [4]. The composite Higgs Lagrangian is a low energy effective theory and higher dimensional operators will also be phenomenologically relevant.

12.4.2.2 The non-linearly realized effective theory

One can always organize the low energy effective theory in a derivative expansion. The best way is to make use of the exponential map

$$U = \exp\left(i\frac{\Pi^a X^a}{F}\right) E\,, \tag{12.27}$$

where Π^a represent the 9 Goldstone bosons and X^a are the 9 generators of $SU(4)$ that do not leave the vacuum invariant. To introduce the electroweak interactions one simply adopts the same covariant derivative used for the linearly realized effective theory, see Eqs. (12.24)–(12.25).

The associated non-linear effective Lagrangian reads

$$L = \frac{F^2}{2}\mathrm{Tr}\left[D_\mu U D^\mu U^\dagger\right] - \frac{1}{2}\Pi_a (M^2_{\mathrm{ETC}})^{ab}\Pi_b\,. \tag{12.28}$$

Still the mass squared matrix parametrizes our ignorance about the underlying ETC dynamics.

A common ETC mass for all the pseudo Goldstone bosons carrying baryon number can be provided by adding the following term to the previous Lagrangian

$$2C\mathrm{Tr}\left[UBU^\dagger B\right] + C = \frac{C}{4F^2}\sum_{i=1}^{6}\Pi^i_B\Pi^i_B\,, \quad \text{with} \quad B = \frac{1}{2\sqrt{2}}\begin{pmatrix} \mathbb{1} & 0 \\ 0 & -\mathbb{1} \end{pmatrix}. \tag{12.29}$$

Dimensional analysis requires $C \propto \Lambda^6_{TC}/\Lambda^2_{ETC}$. A similar term can be added to the linearly realized version of our theory.

[4] We have provided supporting arguments for this picture in [10] where the reader will find also a more general discussion of this issue and possible pitfalls.

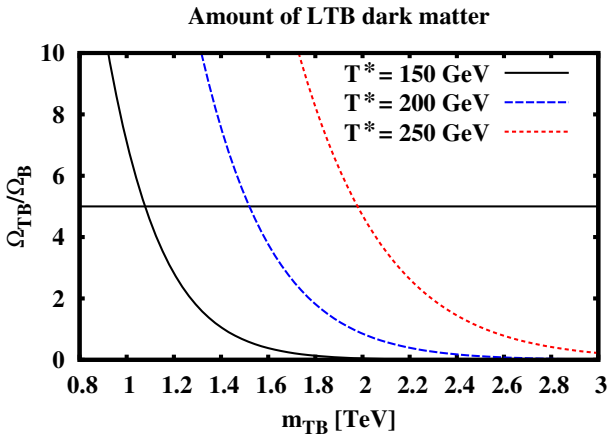

Fig. 12.13: The fraction of technibaryon matter density over the baryonic one as function of the technibaryon mass. The desired value of $\Omega_{TB}/\Omega_B \sim 5$ depends on the lightest technibaryon mass and the value of T^*.

12.4.3 The dark-side of the 5th force

According to the choice of the hypercharge there are two distinct possibilities for a dark matter candidate. If we assume the SM-like hypercharge assignment for the techniquarks and the new lepton family, the new heavy neutrino can be an interesting dark matter candidate. For that, it must be made sufficiently stable by requiring no flavor mixing with the lightest generations and be lighter than the unstable charged lepton [10]. This possibility is currently under investigation [128]. However, we can also consider another possibility. We can choose the hypercharge assignment in such a way that one of the pseudo Goldstone bosons does not carry electric charge. The dynamics providing masses for the pseudo Goldstone bosons may be arranged in a way that the neutral pseudo Goldstone boson is the LTB. If conserved by ETC interactions the technibaryon number protects the lightest baryon from decaying. Since the masses of the technibaryons are of the order of the electroweak scale, they may constitute interesting sources of dark matter. Some time ago in a pioneering work Nussinov [129] suggested that, in analogy with the ordinary baryon asymmetry in the Universe, a technibaryon asymmetry is a natural possibility. A new contribution to the mass of the Universe then emerges due to the presence of the LTB. It is useful to compare the fraction of technibaryon mass Ω_{TB} to baryon mass Ω_B in the Universe

$$\frac{\Omega_{TB}}{\Omega_B} = \frac{TB}{B}\frac{m_{TB}}{m_p}\,, \tag{12.30}$$

where m_p is the proton mass, m_{TB} is the mass of the LTB. TB and B are the technibaryon and baryon number densities, respectively.

Knowing the distribution of dark matter in the galaxy, earth based experiments can set stringent limits on the physical features of the dominant component of dark matter [130]. Such a distribution, however, is not known exactly [131] and it depends on the number of components and type of dark matter. In order to determine few features of our LTB particle we make the oversimplified approximation in which our LTB constitutes the whole dark matter contribution to the mass of the Universe. In this limit the previous ratio should be around 5 [132]. By choosing in our model the hypercharge assignment $y = 1$ the lightest neutral Goldstone boson is the state consisting of the DD techniquarks. The fact that it is charged under $SU(2)_L$ makes it probably detectable in Ge detectors [133].

It is well known that weak anomalies violate the baryon and the lepton number. More precisely, weak processes violate $B + L$, while they preserve $B - L$. Similarly, the weak anomalies violate also the technibaryon number, since technibaryons couple weakly. The weak technibaryon-, lepton- and baryon- number violating effects are highly suppressed at low temperatures while they are enhanced at

temperatures comparable to the critical temperature of the electroweak phase transition [134]. With T^* we define the temperature below which the sphaleron processes cease to be important. This temperature is not exactly known but it is expected to be in the range between $150 - 250$ GeV [134].

Following early analysis [135, 136] we have performed a careful computation of Ω_{TB}/Ω_B within our model. Imposing thermal equilibrium, electric neutrality condition and the presence of a continuous electroweak phase transition (T^* now is below the critical temperature) we find:

$$\frac{TB}{B} = \frac{11}{36}\,\sigma_{TB}\left(\frac{m_{TB}}{T^*}\right)\,, \tag{12.31}$$

with σ_{TB} the statistical weight function

$$\sigma_{TB}\left(\frac{m_{TB}}{T^*}\right) = \frac{3}{2\pi^2}\int_0^\infty dx\; x^2 \sinh^{-2}\left(\frac{1}{2}\sqrt{x^2+\left(\frac{m_{TB}}{T^*}\right)^2}\right)\,. \tag{12.32}$$

In the previous estimate (12.31) the LTB is taken to be lighter then the other technibaryons and the new lepton number is violated. We have, however, considered different scenarios and various limits which will be reported in [137]. Our results are shown in Fig. 12.13. The desired value of the dark matter fraction in the Universe can be obtained for a LTB mass of the order of a TeV for quite a wide range of values of T^*. The only free parameter in our analysis is essentially the mass of the LTB which is ultimately provided by ETC interactions.

12.5 Associate production of a light composite Higgs at the LHC

Alfonso R. Zerwekh

Very recently a new kind of technicolor models has been proposed [10] whose main characteristic is that technifermions are not in the fundamental representation of the technicolor group. In these models the walking behavior of the coupling constant appears naturally and they are not in conflict with the current limits on the oblique parameters. But the most remarkable feature of these models is that they predict the existence of a light composite Higgs with a mass around 150 GeV.

Inspired by such models, we write down an effective Lagrangian which describes the Standard Model with a light Higgs and vector resonances [78] which are a general prediction of dynamical symmetry breaking models [138]. The model is minimal in the sense that we assume that any other composite state would be heavier than the vector resonances, and so they are not taken into account, and there are no physical technipions in the spectrum.

We start by noticing that, in general, dynamical electroweak symmetry breaking models predict the existence of composite vector particles (the so called technirho and techniomega) that mix with the gauge bosons of the Standard Model. In order to describe this mixing, we use a generalization of Vector Meson Dominance [139] introduced in [63] and developed in [140]. In this approach we choose a representation where all vector fields transform as gauge fields and mix through a mass matrix. On the other hand, gauge invariance imposes that the mass matrix has a null determinant. In our case, the Lagrangian for the gauge sector can be written as:

$$\begin{aligned}\mathcal{L} &= -\frac{1}{4}W^a_{\mu\nu}W^{a\mu\nu} - \frac{1}{4}\tilde{\rho}^a_{\mu\nu}\tilde{\rho}^{a\mu\nu} + \frac{M^2}{2}\left(\frac{g^2}{g_2^2}W^a_\mu W^{a\mu} + \tilde{\rho}^a_\mu\tilde{\rho}^{a\mu} - \frac{2g}{g_2}W^a_\mu\tilde{\rho}^{a\mu}\right)\\ &\quad -\frac{1}{4}B_{\mu\nu}B^{\mu\nu} - \frac{1}{4}\tilde{\omega}_{\mu\nu}\tilde{\omega}^{\mu\nu} + \frac{M'^2}{2}\left(\frac{g'^2}{g_2'^2}B_\mu B^\mu + \tilde{\omega}_\mu\tilde{\omega}^\mu - \frac{2g'}{g_2'}B_\mu\tilde{\omega}^\mu\right)\end{aligned} \tag{12.33}$$

Notice that our Lagrangian is written in terms of non-physical fields. The physical ones will be obtained by diagonalizing the mass matrix.

By construction, Lagrangian (12.33) is invariant under $SU(2)_{\rm L} \times U(1)_{\rm Y}$. The symmetry breaking to $U(1)_{\rm em}$ will be described by mean of the vacuum expectation value of a scalar field, as in the Standard Model. In other words, we will use an effective gauged linear sigma model as a phenomenological description of the electroweak symmetry breaking.

As usual, fermions are minimally coupled to gauge bosons through a covariant derivative. Because in our scheme all the vector bosons transform as gauge fields, it is possible to include the proto-technirho and the proto-techniomega in an "extended" covariant derivative [140], resulting in the following Lagrangian for the fermion sector:

$$\mathcal{L} = \bar{\psi_L} i\gamma^\mu D_\mu \psi_L + \bar{\psi_R} i\gamma^\mu \tilde{D}_\mu \psi_R \tag{12.34}$$

with

$$D_\mu = \partial_\mu + i\tau^a g(1-x_1)W^a_\mu + i\tau^a g_2 x_1 \tilde{\rho}^a_\mu + i\frac{Y}{2}g'(1-x_2)B_\mu + i\frac{Y}{2}g'_2 x_2 \tilde{\omega}_\mu$$

and

$$\tilde{D}_\mu = \partial_\mu + i\frac{Y}{2}g'(1-x_3)B_\mu + i\frac{Y}{2}g'_2 x_3 \tilde{\omega}_\mu \tag{12.35}$$

Although a direct coupling between fermions and the vector resonances can appear naturally in technicolor due to extended technicolor interactions we will set $x_i = 0$ ($i = 1, 2, 3$), for simplicity.

In our effective model the Higgs sector is assumed to be the same as in the Standard Model. We avoid the possibility of a direct coupling between the vector resonances and the Higgs because, in principle, it can introduce dangerous tree level corrections to the ρ parameter.

Once the electroweak symmetry has been broken, the mass matrix of the vector bosons takes contributions from (12.33) and from the Higgs mechanism. For the neutral vector bosons, the resulting mass matrix is (written in the basis $(W^3, \tilde{\rho}^3, B, \tilde{\omega})$ and assuming $M' = M$ and $g'_2 = g_2$):

$$\mathcal{M}_{\rm neutral} = \frac{v^2}{4}\begin{bmatrix} (1+\alpha)g^2 & -\alpha g g_2 & -gg' & 0 \\ -\alpha g g_2 & \alpha g_2^2 & 0 & 0 \\ -gg' & 0 & (1+\alpha)g'^2 & -\alpha g' g_2 \\ 0 & 0 & -\alpha g' g_2 & \alpha g'^2 \end{bmatrix} \tag{12.36}$$

where $\alpha = \frac{4M^2}{v^2 g_2^2}$.

On the other hand, the mass matrix for the charged vector bosons can be written as(written in the basis $(\tilde{W}^+, \tilde{\rho}^+)$ where $\tilde{W}^+ = (W^1 - iW^2)/\sqrt{2}$ and $\tilde{\rho}^+ = (\tilde{\rho}^1 - i\tilde{\rho}^2)/\sqrt{2}$):

$$\mathcal{M}_{\rm charged} = \frac{v^2}{4}\begin{bmatrix} (1+\alpha)g^2 & -\alpha g g_2 \\ -\alpha g g_2 & \alpha g_2^2 \end{bmatrix} \tag{12.37}$$

After diagonalizing the mass matrix we can write the interactions in terms of the physical fields. The relevant Feynman rules for the associate production of a Higgs and a gauge boson, in the limit $g/g_2 \ll 1$, can be found in Table 12.1.

We compute the cross section of the associate production of a Higgs and a gauge boson at the LHC. We choose to work with $\alpha = 0.1$ because for values of α of this order, the vector resonances can be light (i.e. $M_\rho \approx 250$ GeV) while g_2/g is still much bigger than one. As α approaches unity, the vector resonances became too heavy and their observation increasingly difficult. On the other hand, if α is too small the coupling of the vector resonances to the SM fields are suppressed.

In Fig. 12.14 we show the value of $(\sigma - \sigma_{\rm SM})/\sigma_{\rm SM}$ as a function of the mass of the technirho (M_ρ) for three values of the Higgs mass ($M_H = 115$ GeV (solid line),150 GeV (dashed line) and 200 GeV (dotted line)) for the process $pp \to HW^+$ at the LHC. Observe that in this case, the cross section is significatively enhanced with respect to the Standard Model when the technirho has a mass between

Table 12.1: Feynman Rules for the relevant couplings of the vector resonances for the associated production of a Higgs and a gauge bosons. The couplings of the $W^{\pm}$ and Z to the quarks are identical, in our limit, to the SM.

Fields in the vertex	Variational derivative of Lagrangian by fields
$H\ \omega_\mu^0\ Z_\nu$	$\frac{1}{2}\frac{e^2 M_W\sqrt{\alpha}v}{{c_w}^3 M_\rho} g^{\mu\nu}$
$H\ \rho_\mu^0\ Z_\nu$	$-\frac{1}{2}\frac{e^2 M_W\sqrt{\alpha}v}{{c_w}^2 M_\rho s_w} g^{\mu\nu}$
$H\ \rho_\mu^+\ {W^-}_\nu$	$-\frac{1}{2}\frac{e^2 M_W\sqrt{\alpha}v}{M_\rho {s_w}^2} g^{\mu\nu}$
$\bar{u}\ d\ \rho_\mu^+$	$\frac{1}{8}\frac{e^2\sqrt{2}\sqrt{\alpha}V_{ud}v}{M_\rho {s_w}^2}(1-\gamma^5)\gamma^\mu$
$\bar{u}\ u\ \omega_\mu^0$	$\frac{1}{24}\frac{e^2\sqrt{\alpha}v}{{c_w}^2 M_\rho}\gamma^\mu\big((1-\gamma^5)+4(1+\gamma^5)\big)$
$\bar{u}\ u\ \rho_\mu^0$	$\frac{1}{8}\frac{e^2\sqrt{\alpha}v}{c_w M_\rho s_w}(1-\gamma^5)\gamma^\mu$

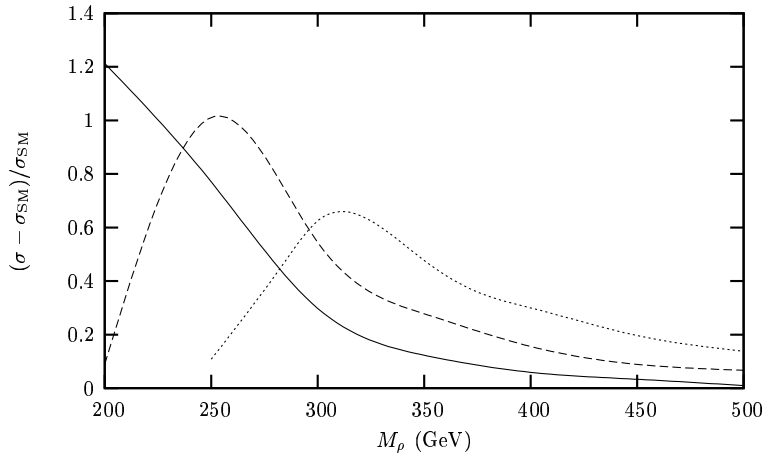

Fig. 12.14: Enhancement of the cross section, $(\sigma-\sigma_{\rm SM})/\sigma_{\rm SM}$, in the process $pp\to W^+H$ at the LHC for three values of the Higgs mass: $M_H=115$ GeV (solid line), 150 GeV (dashed line) and 200 GeV (dotted line). In all cases we took $\alpha=0.1$.

200 GeV and 350 GeV. The variation of this enhancement as a function of α is shown in Fig. 12.15 for $M_H=150$ GeV and $g_2/g=10$. On the other hand, when a Higgs and a Z are produced (Fig. 12.16), the cross section is less enhanced and we expect that this channel will not be sensible to the presence of the vector resonances.

The point in the parameter space we use for studying our model was chosen in order to maximize the deviation from the Standard Model for the selected channel. This procedure allows us to evaluate the possibility of testing the model. Unfortunately, this point is disfavored by precision measurements. Nevertheless, we can be consistent with the constrains imposed by precision data by choosing $x_1=2(g/g_2)^2$ in (12.34). In this case, our results on $\sigma-\sigma_{\rm SM}$ are modified by a factor 0.60 and an important enhancement remains in the channel $pp\to HW^+$ for M_ρ around 250 GeV.

In conclusion, we have constructed an effective Lagrangian which represents the Standard Model with a light (composite) Higgs boson and vector resonances that mix with the gauge bosons. We fixed the parameter of the model that connects the mass of the new vector bosons with their coupling constant, in such a way that the model is compatible with light resonances. The most obvious process for searching differences between our model and the predictions of the Standard Model is the associate production of a Higgs and a gauge boson. We found that the most sensitive channel is the production of the Higgs and W.

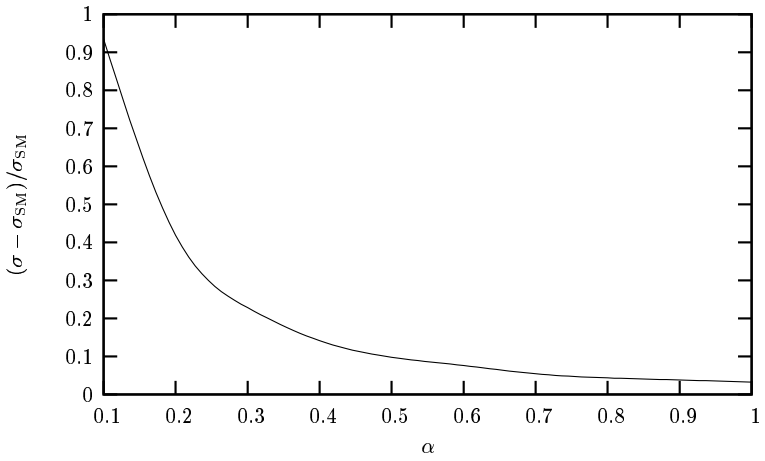

Fig. 12.15: Enhancement of the cross section in the process $p\bar{p} \to W^+H$ at the LHC as a function of α for $M_H = 150$ GeV and $g/g_2 = 0.1$.

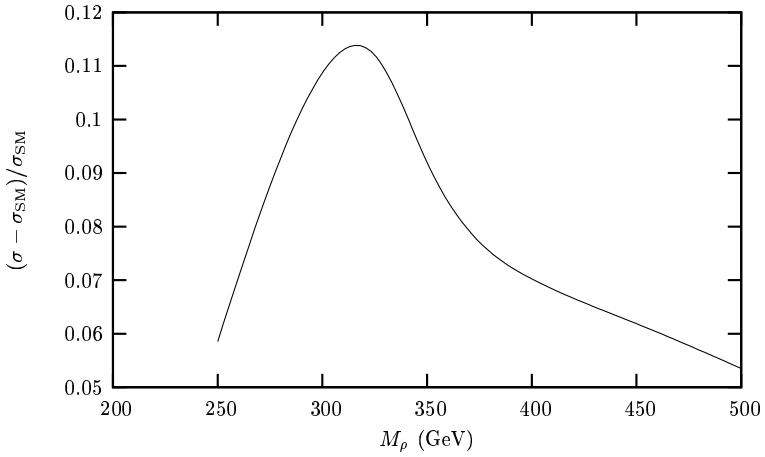

Fig. 12.16: Enhancement of the cross section in the process $pp \to ZH$ at the LHC for $M_H = 200$ GeV.

For a range of resonance's mass between 200 GeV and 350 GeV the enhancement of the cross section is significant at the LHC, depending on the Higgs mass. A relative light Higgs ($M_H = 115$ GeV) would be sensible to a technirho with mass between 200 GeV and 270 GeV while the production of a heavier Higgs ($M_H = 200$ GeV) would be enhanced by the presence of a technirho with a mass around 320 GeV.

12.6 Towards understanding the nature of electroweak symmetry breaking at hadron colliders: distinguishing technicolor and supersymmetry.

Alexander Belyaev

Many alternative models of electroweak symmetry breaking have spectra that include new scalar or pseudoscalar states whose masses could easily lie in the range to which Run II is sensitive. The new scalars tend to have cross-sections and branching fractions that differ from those of the SM Higgs. Here we discuss how to extract information about non-Standard theories of electroweak symmetry breaking from searches for a light SM Higgs at Tevatron Run II and CERN LHC. Ref. [141] studied the potential of Tevatron Run II to augment its search for the SM Higgs boson by considering the process $gg \to h_{SM} \to \tau^+\tau^-$. Authors determined what additional enhancement of scalar production and branching rate would

enable a scalar to become visible in the $\tau^+\tau^-$ channel alone at Tevatron Run II. Similar work has been done for $gg \to h_{MSSM} \to \tau^+\tau^-$ at the LHC [142] and for $gg \to h_{SM} \to \gamma\gamma$ at the Tevatron [143] and LHC [144].

This contribution builds on these results and studies enhanced signals from (pseudo)scalar production in dynamical electroweak symmetry and supersymmetry considering an additional production mechanism (b-quark annihilation), more decay channels ($b\bar{b}$, W^+W^-, ZZ, and $\gamma\gamma$). We suggest the mass reach of the standard Higgs searches for each kind of non-standard scalar state. We also compare the key signals for the non-standard scalars across models and also with expectations in the SM, to show how one could identify which state has actually been found.

12.6.1 Models of electroweak symmetry breaking

12.6.1.1 Supersymmetry

One interesting possibility for addressing the hierarchy and triviality problems of the Standard Model is to introduce supersymmetry. In order to provide masses to both up-type and down-type quarks, and to ensure anomaly cancellation, the MSSM contains two Higgs complex-doublet superfields: $\Phi_d = (\Phi_d^0, \Phi_d^-)$ and $\Phi_u = (\Phi_u^+, \Phi_u^0)$ which aquire two vacuum expectation values v_1 and v_2 respectively. Out of the original 8 degrees of freedom, 3 serve as Goldstone bosons, absorbed into longitudinal components of the $W^\pm$ and Z, making them massive. The other 5 degrees of freedom remain in the spectrum as distinct scalar states, namely two neutral CP-even states(h, H), one neutral, CP-odd state (A) and a charged pair ($H^\pm$). It is conventional to choose $\tan\beta = v_1/v_2$ and $M_A = \sqrt{M_{H^\pm}^2 - M_W^2}$ to define the SUSY Higgs sector. There are following tree-level relations between Higgs masses which will be useful for understanding enhanced Higgs boson interactions with fermions:

$$M_{h,H}^2 = \frac{1}{2}\left[(M_A^2 + M_Z^2) \mp \sqrt{(M_A^2 + M_Z^2)^2 - 4M_A^2 M_Z^2 \cos^2 2\beta}\right],$$
$$\cos^2(\beta - \alpha) = \frac{M_h^2(M_Z^2 - M_h^2)}{M_A^2(M_H^2 - M_h^2)}, \tag{12.38}$$

where α is the mixing angle of CP-even Higgs bosons. The Yukawa interactions of the Higgs fields with the quarks and leptons can be written as:

$$\begin{aligned} Y_{ht\bar{t}}/Y_{ht\bar{t}}^{SM} &= \cos\alpha/\sin\beta, & Y_{Ht\bar{t}}/Y_{ht\bar{t}}^{SM} &= \sin\alpha/\sin\beta, & Y_{At\bar{t}}/Y_{ht\bar{t}}^{SM} &= \cot\beta, \\ Y_{hb\bar{b}}/Y_{hb\bar{b}}^{SM} &= -\sin\alpha/\cos\beta, & Y_{Hb\bar{b}}/Y_{hb\bar{b}}^{SM} &= \cos\alpha/\cos\beta, & Y_{Ab\bar{b}}/Y_{hb\bar{b}}^{SM} &= \tan\beta, \end{aligned} \tag{12.39}$$

relative to the Yukawa couplings of the Standard Model ($Y_{hf\bar{f}}^{SM} = m_f/v$). Once again, the same pattern holds for the tau lepton's Yukawa couplings as for those of the b quark. There are several circumstances under which various Yukawa couplings are enhanced relative to Standard Model values. For high $\tan\beta$ (small $\cos\beta$), Eqs. (12.39) show that the interactions of all neutral Higgs bosons with the down-type fermions are enhanced by a factor of $1/\cos\beta$. In the decoupling limit, where $M_A \to \infty$, applying Eq. (12.38) to Eqs. (12.39) shows that the H and A Yukawa couplings to down-type fermions are enhanced by a factor of $\simeq \tan\beta$. Conversely, for low $M_A \simeq M_h$, one can check that $Y_{hb\bar{b}}/Y_{hb\bar{b}}^{SM} = Y_{h\tau\bar{\tau}}/Y_{h\tau\bar{\tau}}^{SM} \simeq \tan\beta$ and that h and A Yukawas are enhanced instead.

12.6.1.2 Technicolor

Another intriguing class of theories, dynamical electroweak symmetry breaking (DEWSB), supposes that the scalar states involved in electroweak symmetry breaking could be manifestly composite at scales not much above the electroweak scale $v \sim 250$ GeV. In these theories, a new asymptotically free strong gauge interaction (technicolor [1, 2, 145]) breaks the chiral symmetries of massless fermions f at a scale $\Lambda \sim 1$ TeV. If the fermions carry appropriate electroweak quantum numbers (e.g. left-hand (LH) weak doublets

and right-hand (RH) weak singlets), the resulting condensate $\langle \bar{f}_L f_R \rangle \neq 0$ breaks the electroweak symmetry as desired. Three of the Nambu-Goldstone Bosons (technipions) of the chiral symmetry breaking become the longitudinal modes of the W and Z. The logarithmic running of the strong gauge coupling renders the low value of the electroweak scale natural. The absence of fundamental scalars obviates concerns about triviality. For details, we refer the reader to section 12.1.

Many models of DEWSB have additional light neutral pseudo Nambu-Goldstone bosons which could potentially be accessible to a standard Higgs search; these are called "technipions" in technicolor models. Our analysis will assume, for simplicity, that the lightest PNGB state is significantly lighter than other neutral (pseudo) scalar technipions, so as to heighten the comparison to the SM Higgs boson. The specific models we examine are: 1) the traditional one-family model [146] with a full family of techniquarks and technileptons, 2) a variant on the one-family model [147] in which the lightest technipion contains only down-type technifermions and is significantly lighter than the other pseudo Nambu-Goldstone bosons, 3) a multiscale walking technicolor model [37] designed to reduce flavor-changing neutral currents, and 4) a low-scale technicolor model (the Technicolor Straw Man model) [53] with many weak doublets of technifermions, in which the second-lightest technipion P' is the state relevant for our study (the lightest, being composed of technileptons, lacks the anomalous coupling to gluons required for $gg \to P$ production). For simplicity the lightest relevant neutral technipion of each model will be generically denoted P; where a specific model is meant, a superscript will be used. One of the key differences among these models is the value of the technipion decay constant F_P, which is related to the number N_D of weak doublets of technifermions that contribute to electroweak symmetry breaking. We refer the reader to [148] for details.

12.6.2 Results for each model

12.6.2.1 Supersymmetry

Let us consider how the signal of a light Higgs boson could be changed in the MSSM, compared to expectations in the SM. There are several important sources of alterations in the predicted signal, some of which are interconnected. First, the MSSM includes three neutral Higgs bosons $\mathcal{H} = (h, H, A)$ states. The apparent signal of a single light Higgs could be enhanced if two or three neutral Higgs species are nearly degenerate. Second, the alterations of the couplings between Higgs bosons and ordinary fermions in the MSSM can change the Higgs decay widths and branching ratios relative to those in the SM. Radiative effects on the masses and couplings can substantially alter decay branching fractions in a non-universal way. For instance, $B(h \to \tau^+\tau^-)$ could be enhanced by up to an order of magnitude due to the suppression of $B(h \to b\bar{b})$ in certain regions of parameter space [149, 150]. However, this gain in branching fraction would be offset to some degree by a reduction in Higgs production through channels involving $Y_{\mathcal{H}b\bar{b}}$ [141]. Third, a large value of $\tan\beta$ enhances the bottom-Higgs coupling (Eqs. (12.39)), making gluon fusion through a b-quark loop significant, and possibly even dominant over the top-quark loop contribution. Fourth, the presence of superpartners in the MSSM gives rise to new squark-loop contributions to Higgs boson production through gluon fusion. Light squarks with masses of order 100 GeV have been argued to lead to a considerable universal enhancement (as much as a factor of five) [151–154] for MSSM Higgs production compared to the SM. Finally, enhancement of the $Y_{\mathcal{H}b\bar{b}}$ coupling at moderate to large $\tan\beta$ makes $b\bar{b} \to \mathcal{H}$ a significant means of Higgs production in the MSSM – in contrast to the SM where it is negligible. To include both production channels when looking for a Higgs decaying as $\mathcal{H} \to xx$, we define a combined enhancement factor

$$\kappa^{\mathcal{H}}_{total/xx} = \frac{\sigma(gg \to \mathcal{H} \to xx) + \sigma(bb \to \mathcal{H} \to xx)}{\sigma(gg \to h_{SM} \to xx) + \sigma(bb \to h_{SM} \to xx)} \equiv [\kappa^{\mathcal{H}}_{gg/xx} + \kappa^{\mathcal{H}}_{bb/xx} R_{bb:gg}]/[1 + R_{bb:gg}]. \tag{12.40}$$

Here $R_{bb:gg}$ is the ratio of $b\bar{b}$ and gg initiated Higgs boson production in the Standard Model, which can be calculated using HDECAY.

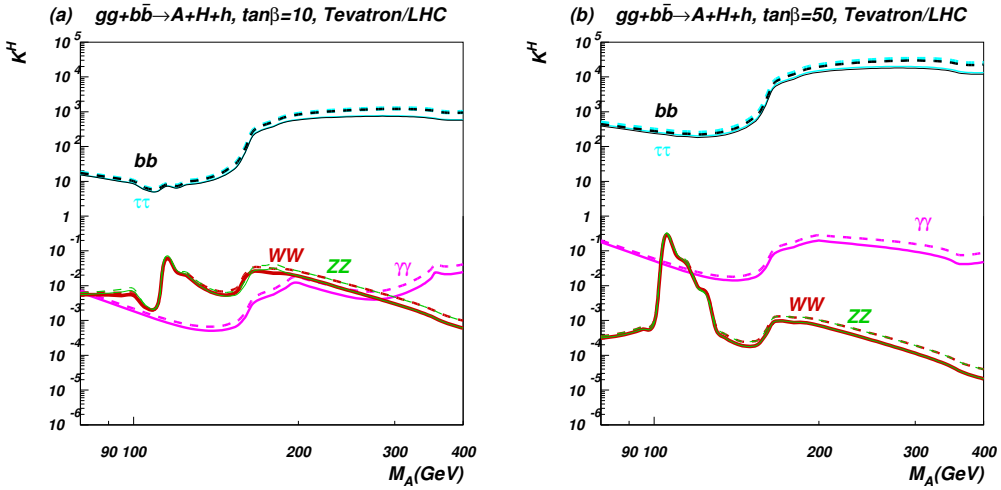

Fig. 12.17: Enhancement factor $\kappa^{\mathcal{H}}_{tot/xx}$ for final states $xx = b\bar{b},\ \tau^+\tau^-,\ WW,\ ZZ,\ \gamma\gamma$ when both $gg \to \mathcal{H}$ and $b\bar{b} \to \mathcal{H}$ are included and the signals of all three MSSM Higgs states are combined. Frames (a) and (b) correspond to $\tan\beta = 10$ and 50, respectively, at the Tevatron (solid lines) and at the LHC (dashed lines).

In the MSSM the contribution from $b\bar{b} \to \mathcal{H}$ becomes important even for moderate values of $\tan\beta \sim 10$ and both, $b\bar{b} \to \mathcal{H}$ and $gg \to \mathcal{H}$ productions are significantly enchanced with $\tan\beta$ compared to the SM rates [148]. For $M_{\mathcal{H}} < 110 - 115$ GeV the contribution from $gg \to \mathcal{H}$ process is a bit bigger than that from $b\bar{b} \to \mathcal{H}$, while for $M_{\mathcal{H}} > 115$ GeV b-quark-initiated production begins to outweigh gluon-initiated production. Results for LHC are qualitatively similar, except the rate, which is about two orders of magnitude higher compared to that at the Tevatron. Using the Higgs branching fractions with these NLO cross sections for $gg \to H$ and $b\bar{b} \to H$ allows us to derive $\kappa^{\mathcal{H}}_{total/xx}$, as presented in Fig. 12.17 for the Tevatron and LHC. There are several "physical" kinks and peaks in the enhancement factor for various Higgs boson final states related to WW, ZZ and top-quark thresholds which can be seen for the respective values of M_A. At very large values of $\tan\beta$ the top-quark threshold effect for the $\gamma\gamma$ enhancement factor is almost gone because the b-quark contribution dominates in the loop. One can see from Fig. 12.17 that the enhancement factors at the Tevatron and LHC are very similar. In contrast to strongly enhanced $b\bar{b}$ and $\tau\bar{\tau}$ signatures, the $\gamma\gamma$ signature is always strongly suppressed! This particular feature of SUSY models, as we will see below, may be important for distinguishing supersymmetric models from models with dynamical symmetry breaking. It is important to note that combining the signals from A, h, H has the virtue of making the enhancement factor independent of the degree of top squark mixing (for fixed M_A, μ and M_S and medium to high values of $\tan\beta$), which greatly reduces the parameter-dependence of our results.

12.6.2.2 Technicolor

Single production of a technipion can occur through the axial-vector anomaly which couples the technipion to pairs of gauge bosons. For an $SU(N_{TC})$ technicolor group with technipion decay constant F_P, the anomalous coupling between the technipion and a pair of gauge bosons is given, in direct analogy with the coupling of a QCD pion to photons, by [155–157]. Comparing a PNGB to a SM Higgs boson of the same mass, we find the enhancement in the gluon fusion production is

$$\kappa_{gg\ prod} = \frac{\Gamma(P \to gg)}{\Gamma(h \to gg)} = \frac{9}{4} N_{TC}^2 \mathcal{A}_{gg}^2 \frac{v^2}{F_P^2} \tag{12.41}$$

The main factors influencing $\kappa_{gg\ prod}$ for a fixed value of N_{TC} are the anomalous coupling to gluons and the technipion decay constant. The value of κ_{prod} for each model (taking $N_{TC} = 4$) is given in

Table 12.2: Enhancement Factors for 130 GeV technipions produced at the Tevatron and LHC, compared to production and decay of a SM Higgs Boson of the same mass. The slight suppression of κ^P_{prod} due to the b-quark annihilation channel has been included. The rightmost column shows the cross-section (pb) for $p\bar{p}/pp \to P \to xx$ at Tevatron Run II/LHC.

Model	Decay mode	κ^P_{prod}	κ^P_{dec}	$\kappa^P_{tot/xx}$	σ(pb) Tevatron/LHC
1) one family	$b\bar{b}$	47	1.1	52	14 / 890
	$\tau^+\tau^-$	47	0.6	28	0.77 / 48
	$\gamma\gamma$	47	0.12	5.6	6.4×10^{-3} / 0.4
2) variant one family	$b\bar{b}$	5.9	1	5.9	1.8 / 100
	$\tau^+\tau^-$	5.9	5	30	0.84 / 52
	$\gamma\gamma$	5.9	1.3	7.7	8.7×10^{-3} / 0.55
3) multiscale	$b\bar{b}$	1100	0.43	470	130 / 8000
	$\tau^+\tau^-$	1100	0.2	220	6.1 / 380
	$\gamma\gamma$	1100	0.27	300	0.34 /22
4) low scale	$\tau^+\tau^-$	120	0.6	72	2/120
	$\gamma\gamma$	120	2.9	350	0.4/25

Table 12.2. One should note, that the value of $\kappa_{bb\ prod}$ is at least one order of magnitude smaller than $\kappa_{gg\ prod}$ in each model. From the $\kappa_{gg\ prod}/\kappa_{bb\ prod}$ ratio which reads as

$$\frac{\kappa_{gg\ prod}}{\kappa_{bb\ prod}} = \frac{9}{4} N_{TC}^2 \mathcal{A}_{gg}^2 \lambda_b^{-2} \left(1 - \frac{4m_b^2}{m_h^2}\right)^{\frac{3-s}{2}}, \tag{12.42}$$

we see that the larger size of $\kappa_{gg\ prod}$ is due to the factor of N_{TC}^2 coming from the fact that gluons couple to a technipion via a techniquark loop. Technicolor models with a large number of techniquarks are in quite a tension with the precision data. However the recent Technicolor models with two technicolors and only two Dirac technifermions in the adjoint representation of the Technicolor gauge group [35] are in better agreement with the precision electroweak measurements. The extended technicolor (ETC) interactions coupling b-quarks to a technipion have no such enhancement. With a smaller SM cross-section and a smaller enhancement factor, it is clear that technipion production via $b\bar{b}$ annihilation is essentially negligible at these hadron colliders. Comparing the technicolor and SM branching ratios in, we see immediately that all decay enhancements are of the order of one. Model 2 is an exception; its unusual Yukawa couplings yield a decay enhancement in the $\tau^+\tau^-$ channel of order the technipion's (low) production enhancement. In the $\gamma\gamma$ channel, the decay enhancement strongly depends on the group-theoretical structure of the model, through the anomaly factor. Our results for the Tevatron Run II and LHC production enhancements (including both gg fusion and $b\bar{b}$ annihilation), decay enhancements, and overall enhancements of each technicolor model relative to the SM are shown in Table 12.2 for a technipion or Higgs mass of 130 GeV. Multiplying $\kappa^P_{tot/xx}$ by the cross-section for SM Higgs production via gluon fusion [158] yields an approximate technipion production cross-section, as shown in the right-most column of Table 12.2.

In each technicolor model, the main enhancement of the possible technipion signal relative to that of an SM Higgs arises at production, making the size of the technipion decay constant the most critical factor in determining the degree of enhancement for fixed N_{TC}.

12.6.3 Interpretation

We are ready to put our results in context. The large QCD background for $q\bar{q}$ states of any flavor makes the tau-lepton-pair and di-photon final states the most promising for exclusion or discovery of the Higgs-

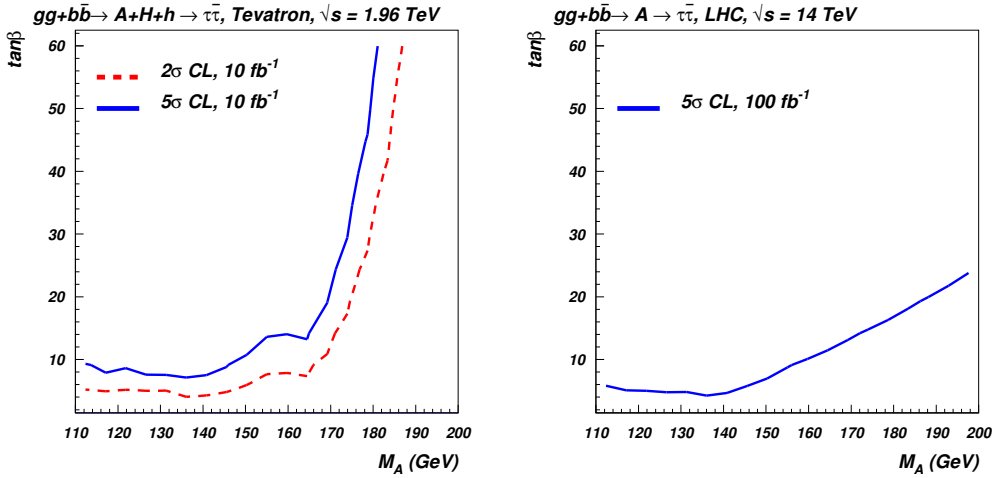

Fig. 12.18: Observability of Supersymmetric Higgs boson production $gg+b\bar{b} \to h+H+A \to \tau^+\tau^-$ for Tevatron (left) and LHC (right). For nearly degenerate Higgs bosons signal is combined in the mass window around M_A (see [148] for details). The parameter space above curves is covered with a given confidence level (CL). The collider reach is based on the $h_{SM} \to \tau^+\tau^-$ studies of [142], in the MSSM parameter space.

like states of the MSSM or technicolor.

In Figure 12.18 we summarize the ability of Tevatron (left) and LHC (right) to explore the MSSM parameter space (in terms of both a 2σ exclusion curve and a 5σ discovery curve) using the process $gg + b\bar{b} \to h + A + H \to \tau^+\tau^-$. Translating the enhancement factors into this reach plot draws on the results of [141]. As the M_A mass increases up to about 140 GeV, the opening of the W^+W^- decay channel drives the $\tau^+\tau^-$ branching fraction down, and increases the $\tan\beta$ value required to make Higgses visible in the $\tau^+\tau^-$ channel. At still larger M_A, a very steep drop in the gluon luminosity (and the related b-quark luminosity) at large x reduces the phase space for $\mathcal{H}$ production. Therefore for M_A >170 GeV, Higgs bosons would only be visible at very high values of $\tan\beta$. The pictures for Tevatron and LHC are qualitatively similar, the main differences compared to the Tevatron are that the required value of $\tan\beta$ at the LHC is lower for a given M_A and it does not climb steeply for M_A >170 GeV because there is much less phase space suppression.

It is important to notice that both, Tevatron and LHC, could observe MSSM Higgs bosons in the $\tau^+\tau^-$ channel even for moderate values of $\tan\beta$ for $M_A \lesssim 200$ GeV, because of significant enhancement of this channel. However the $\gamma\gamma$ channel is so suppressed that even the LHC will not be able to observe it in any point of the $M_A < 200$ GeV parameter space studied in this paper! [5]

The Figure 12.19 presents the Tevatron and LHC potentials to observe technipions. For the Tevatron, the observability is presented in terms of enhancement factor, while for the LHC we present signal rate in term of $\sigma \times Br(P \to \tau\tau/\gamma\gamma)$. At the Tevatron, the available enhancement is well above what is required to render the P of any of these models visible in the $\tau^+\tau^-$ channel. Likewise, the right frame of that figure shows that in the $\gamma\gamma$ channel at the Tevatron the technipions of models 3 and 4 will be observable at the 5σ level while model 2 is subject to exclusion at the 2σ level. The situation at the LHC is even more promising: all four models could be observable at the 5σ level in both the $\tau^+\tau^-$ (left frame) and $\gamma\gamma$ (right frame) channels.

Once a supposed light "Higgs boson" is observed in a collider experiment, an immediate important task will be to identify the new state more precisely, i.e. to discern "the meaning of Higgs" in this

[5] In the decoupling limit with large values of M_A and low values of $\tan\beta$, the lightest MSSM Higgs could be dicovered in the $\gamma\gamma$ mode just like the SM model Higgs boson

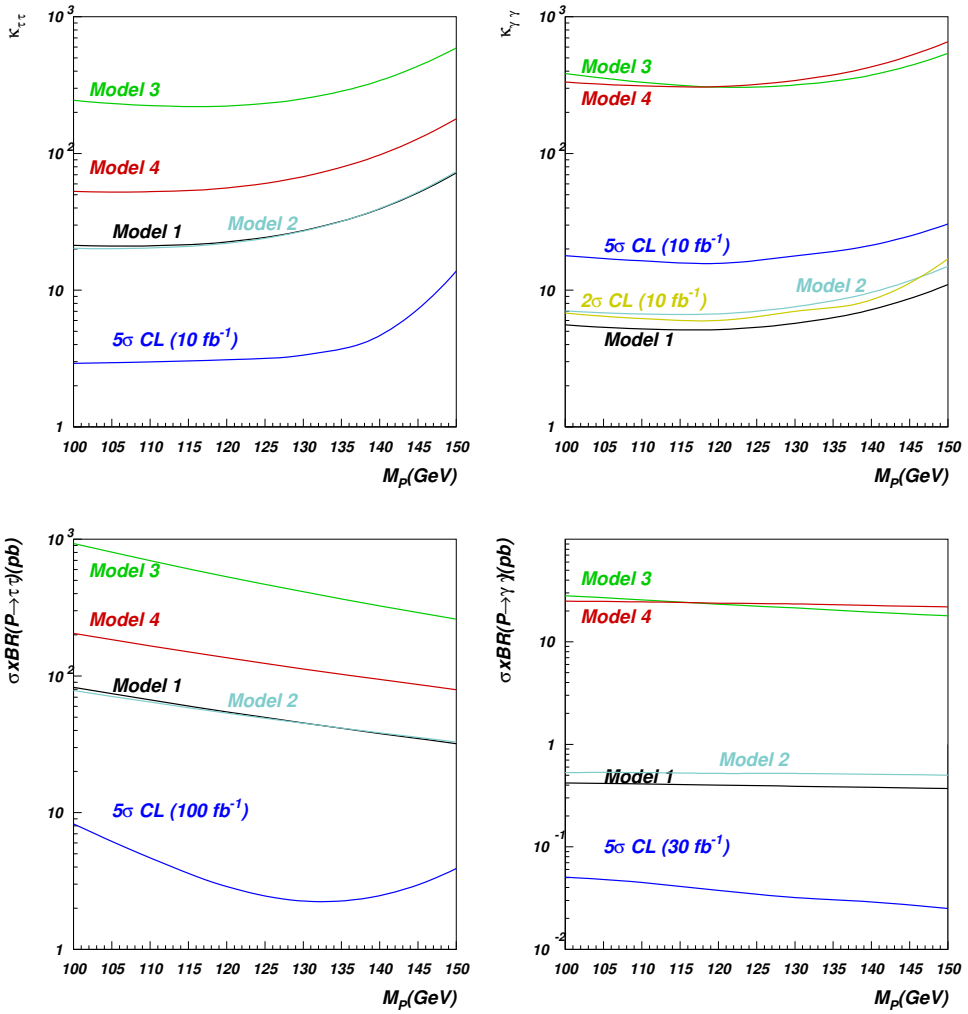

Fig. 12.19: Observability of technipions as a function of technipion mass for tau pair (left frame) or photon pair (right frame) at the Tevatron and LHC in the final state. Top: enhancement factors required for a 5σ discovery and 2σ exclusion for a Higgs-like particle at Tevatron Run II. Bottom: the lowest curve is the $\sigma \times Br$ required to make a Higgs-like particle visible in $\tau^+\tau^-$ or in $\gamma\gamma$ at LHC.

context. Comparison of the enhancement factors for different channels will aid in this task. Our study has shown that comparison of the $\tau^+\tau^-$ and $\gamma\gamma$ channels can be particularly informative in distinguishing supersymmetric from dynamical models. In the case of supersymmetry, when the $\tau^+\tau^-$ channel is enhanced, the $\gamma\gamma$ channel is suppressed, and this suppression is strong enough that even the LHC would not observe the $\gamma\gamma$ signature. In contrast, for the dynamical symmetry breaking models studied we expect *simultaneous* enhancement of both the $\tau^+\tau^-$ and $\gamma\gamma$ channels. The enhancement of the $\gamma\gamma$ channel is so significant, that even at the Tevatron we may observe technipions via this signature at the 5σ level for Models 3 and 4, while Model 2 could be excluded at 95% CL at the Tevatron. The LHC collider, which will have better sensitivity to the signatures under study, will be able to observe all four models of dynamical symmetry breaking studied here in the $\gamma\gamma$ channel, and can therefore distinguish more conclusively between the supersymmetric and dynamical models.

12.6.4 Conclusions

We have shown that searches for a light Standard Model Higgs boson at Tevatron Run II and CERN LHC have the power to provide significant information about important classes of physics beyond the Standard Model. We demonstrated that the new scalar and pseudo-scalar states predicted in both supersymmetric and dynamical models can have enhanced visibility in standard $\tau^+\tau^-$ and $\gamma\gamma$ search channels, making them potentially discoverable at both the Tevatron Run II and the CERN LHC. In comparing the key signals for the non-standard scalars across models we investigated the likely mass reach of the Higgs search in $pp/p\bar{p} \to \mathcal{H} \to \tau^+\tau^-$ for each kind of non-standard scalar state, and we demonstrated that $pp \;\; p\bar{p} \to \mathcal{H} \to \gamma\gamma$ may cleanly distinguish the scalars of supersymmetric models from those of dynamical models.

12.7 Dynamical breakdown of an Abelian gauge chiral symmetry by strong Yukawa couplings [6]

Petr Beneš, Tomáš Brauner and Jiří Hošek

The standard technicolour scenarios [1, 2] dispense with the elementary Higgs and, instead of its vacuum expectation value, generate the order parameter for electroweak symmetry breaking by a bilinear condensate of new fermions. This is bound together by a new strong gauge interaction.

In this contribution we suggest a different mechanism for dynamical electroweak symmetry breaking. The central idea may be summarised as follows. We retain the elementary scalar, but with a positive mass squared so that the usual particle interpretation is preserved even in the absence of interactions. Our basic assumption is the existence of a strong Yukawa interaction between the scalar and the massless fermions. We show that, provided the Yukawa coupling is large enough, the fermion masses may be generated spontaneously as a self-consistent solution of the Schwinger–Dyson equations. In order to make the proposed mechanism more transparent, we demonstrate it on the dynamical breaking of an Abelian chiral symmetry. The extension to the full electroweak $SU(2)_L \times U(1)_Y$ gauge invariance is currently being worked on.

Our plan is the following. First, we recall our previous results and show how a global chiral symmetry may be dynamically broken by a strong Yukawa interaction, thus generating the fermion masses [159]. Second, the axial part of the symmetry is gauged and a sum rule for the gauge boson mass is derived. Last, we explicitly work out the one-loop triple gauge boson vertex as a genuine prediction of the broken symmetry. The extension to the electroweak theory is discussed in the conclusions.

12.7.1 Global chiral symmetry

Following closely our recent paper [159], we consider a model of two Dirac fermions $\psi_{1,2}$ and a complex scalar ϕ, defined by the Lagrangian,

$$\mathcal{L} = \sum_{j=1,2} \left(\bar{\psi}_{jL} i\partial\!\!\!/ \psi_{jL} + \bar{\psi}_{jR} i\partial\!\!\!/ \psi_{jR}\right) + \partial_\mu \phi^\dagger \partial^\mu \phi - M^2 \phi^\dagger \phi - \frac{1}{2}\lambda(\phi^\dagger\phi)^2 + \\ + y_1(\bar{\psi}_{1L}\psi_{1R}\phi + \bar{\psi}_{1R}\psi_{1L}\phi^\dagger) + y_2(\bar{\psi}_{2R}\psi_{2L}\phi + \bar{\psi}_{2L}\psi_{2R}\phi^\dagger). \quad (12.43)$$

The Yukawa couplings y_1, y_2 are assumed real. Note that the Lagrangian (12.43) is invariant under the global Abelian group $U(1)_{V_1} \times U(1)_{V_2} \times U(1)_A$. The two vector $U(1)$'s correspond to independent phase transformations of ψ_1 and ψ_2 i.e., are generated by the operators of the number of fermions of the respective type. The axial $U(1)_A$, on the other hand, relates all the fields included. It consists of transformations of the type

$$\psi_1 \to e^{+i\theta\gamma_5}\psi_1, \quad \psi_2 \to e^{-i\theta\gamma_5}\psi_2, \quad \phi \to e^{-2i\theta}\phi.$$

[6] Although this contribution is not related to technicolor, it is included in this section. It constitutes an exotic example of dynamical breaking of an abelian gauge theory which may one day be used to break the electroweak theory.

The fact that the scalar carries nonzero axial charge will be crucial in the following. Note also that the fermions have opposite charges in order to remove the axial anomaly. While this is a convenience at this stage, where the considered symmetry is global, it will become a theoretical necessity later when it is gauged.

Our goal is to show that at sufficiently strong Yukawa interaction, the axial $U(1)_A$ is spontaneously broken. In the fermion sector this means, of course, that nonzero Dirac masses are generated. Analogously in the scalar sector we find the 'anomalous' axial-charge-violating two-point function $\langle\phi\phi\rangle$. Both these effects are related to each other through one-loop Feynman graphs and both thus have to be analysed simultaneously.

To account for the symmetry breaking in the scalar sector, we introduce the formal doublet

$$\Phi = \begin{pmatrix} \phi \\ \phi^\dagger \end{pmatrix},$$

and work with the matrix propagator $iD(x-y) = \langle 0|T\{\Phi(x)\Phi^\dagger(y)\}|0\rangle$. We use the method of the Schwinger–Dyson equations. For the sake of simplicity we neglect all symmetry-preserving radiative corrections to the fermion and scalar propagators, making the following Ansatz,

$$S^{-1}_{1,2}(p) = \not{p} - \Sigma_{1,2}(p^2), \quad D^{-1}(p) = \begin{pmatrix} p^2 - M^2 & -\Pi(p^2) \\ -\Pi^*(p^2) & p^2 - M^2 \end{pmatrix}.$$

The functions $\Sigma_{1,2}(p^2)$ are the Lorentz-scalar fermion proper self-energies that are responsible for the nonzero masses. Likewise, $\Pi(p^2)$ is the anomalous scalar proper self-energy. The scalar spectrum then consists of two real particles with masses given self-consistently by $M^2_{1,2} = M^2 \pm |\Pi(M^2_{1,2})|^2$.

For the purpose of the numerical computation of the self-energies we perform two additional simplifications. First, we abandon the $\lambda(\phi^\dagger\phi)^2$ interaction. This is because the dynamical symmetry breaking is assumed to happen due to the Yukawa interaction, while the λ term in the Lagrangian serves merely as a perturbative counterterm. Second, we neglect all vertex corrections, thus closing the Schwinger–Dyson hierarchy self-consistently at the propagator level. The fermion and scalar propagators are then determined by the solution of the one-loop equations,

$$\Sigma_{1,p} = iy_1^2 \int \frac{d^4k}{(2\pi)^4} \frac{\Sigma_{1,k}}{k^2 - \Sigma^2_{1,k}} \frac{\Pi_{k-p}}{[(k-p)^2 - M^2]^2 - |\Pi_{k-p}|^2},$$

$$\Sigma_{2,p} = iy_2^2 \int \frac{d^4k}{(2\pi)^4} \frac{\Sigma_{2,k}}{k^2 - \Sigma^2_{2,k}} \frac{\Pi^*_{k-p}}{[(k-p)^2 - M^2]^2 - |\Pi_{k-p}|^2},$$

$$\Pi_p = -\sum_{j=1,2} 2iy_j^2 \int \frac{d^4k}{(2\pi)^4} \frac{\Sigma_{j,k}}{k^2 - \Sigma^2_{j,k}} \frac{\Sigma_{j,k-p}}{(k-p)^2 - \Sigma^2_{j,k-p}}.$$

This set of equations have been solved iteratively in the Euclidean space. We found that a nontrivial solution exists only if the Yukawa couplings are large enough. For $y_1 = y_2$ the critical value is about 80. The typical form of the solution is shown in Fig. 12.20. Our model has the remarkable property that a moderate change of the ratio y_1/y_2 transforms into a tremendous change of the mass ratio. For instance, for $y_1 = 77.4$ and $y_2 = 88$ we find $m_1^2/m_2^2 \approx 10^{-3}$ and the mass ratio seems to fall down to zero as y_1 approaches a critical value about 77. This is alluring and gives us a hope that, when applied to the $SU(2)_L \times U(1)_Y$ gauge theory of electroweak interactions, the present mechanism of dynamical symmetry breaking could provide a natural explanation of the hierarchy of the fermion masses.

12.7.2 Gauge axial symmetry

The next step in our analysis is the gauging of the axial part of the global symmetry. Formally, this is done by replacing the ordinary derivatives in the Lagrangian (12.43) with the covariant ones, $D_\mu\psi_1 =$

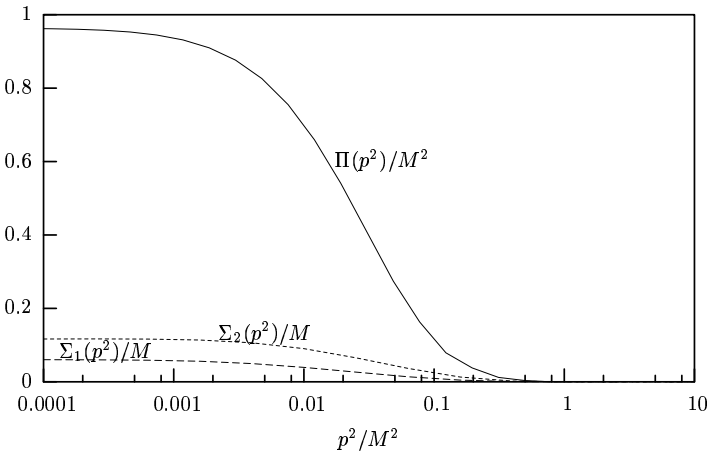

Fig. 12.20: The fermion and scalar proper self-energies for $y_1 = 79$ and $y_2 = 88$.

$(\partial_\mu - igA_\mu\gamma_5)\psi_1$, $D_\mu\psi_2 = (\partial_\mu + igA_\mu\gamma_5)\psi_2$ and $D_\mu\phi = (\partial_\mu + 2igA_\mu)\phi$, and adding the kinetic term for the Abelian gauge field A_μ. We emphasise that the gauge interaction may be switched on perturbatively since it does not play any role in the proposed dynamical mechanism for chiral symmetry breaking.

Once the axial symmetry is spontaneously broken, the gauge boson acquires a nonzero mass through the Schwinger mechanism [160]. Technically, the mass is given by the residue of the massless pole in the gauge boson polarisation tensor.[7] This pole in turn arises from the propagation of the (composite) Goldstone boson of the broken symmetry.

To determine the pole part of the polarisation tensor, one has to know the effective coupling of the Goldstone boson to the axial current or to the gauge boson. First, the axial Ward identity is used to calculate the pole part of the axial current vertex functions, and thus the effective couplings of the Goldstone to the fermions and the scalar [159]. The Goldstone–gauge boson coupling then arises through the fermion and scalar loops. (Recall that the interaction of the fermions and the scalar with the gauge boson is perturbative.) The resulting formula for the dynamically generated gauge boson mass reads $m_A^2 = g^2[I_{\psi_1}(0) + I_{\psi_2}(0) + I_\phi(0)]$, where the one-loop integrals are given by

$$iq^\nu I_{\psi_j}(q^2) = 4\int \frac{d^4k}{(2\pi)^4} \frac{[(k+q)^\nu \Sigma_{j,k} - k^\nu \Sigma_{j,k+q}]\,[\Sigma_{j,k+q} + \Sigma_{ji,k}]}{\left[(k+q)^2 - \Sigma_{j,k+q}^2\right]\left[k^2 - \Sigma_{j,k}^2\right]},$$

$$iq^\nu I_\phi(q^2) = -2\int \frac{d^4k}{(2\pi)^4} \frac{(2k+q)^\nu \left\{(\Pi_{k+q} + \Pi_k)\left[[(k+q)^2 - M^2]\Pi_k^* - (k^2 - M^2)\Pi_{k+q}^*\right] + \text{c.c.}\right\}}{\left\{[(k+q)^2 - M^2]^2 - |\Pi_{k+q}|^2\right\}\left[(k^2 - M^2)^2 - |\Pi_k|^2\right]}.$$

The sample of numerical results is presented in Fig. 12.21.

Note that the gauge boson mass is expressed in terms of the fermion and scalar self-energies by the above one-loop integrals [162]. This clearly distinguishes our model of dynamical symmetry breaking from the standard Higgs mechanism where the fermion and gauge boson masses are generated independently.

12.7.3 Triple gauge boson vertex

The sheer existence of the Goldstone boson and the generation of the gauge boson mass are robust, model-independent predictions of the broken symmetry. In order to achieve deeper insight into the

[7] In fact, this procedure gives only an approximate value of the gauge boson mass, because of the neglected finite part of the polarisation tensor [161]. Such an approximation is justified provided the generated mass is small enough.

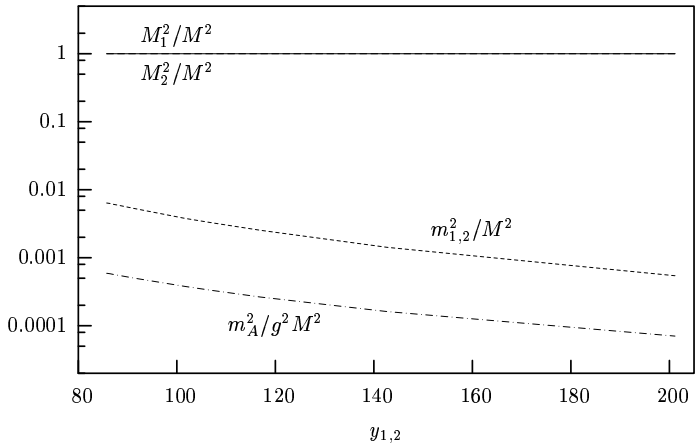

Fig. 12.21: The mass spectrum as a function of $y_1 = y_2$. Here $M_{1,2}, m_{1,2}, m_A$ are the masses of the heavy scalars, the fermions, and the gauge boson, respectively.

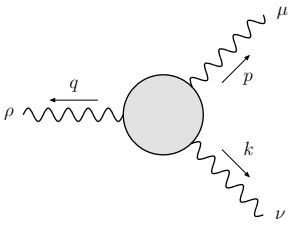

Fig. 12.22: The A^3 vertex, denoted as $iT^{\mu\nu\rho}(p,k)$. There are only two independent momentum variables due to the conservation $p + k + q = 0$.

dynamical origin of the symmetry breaking, it is necessary to work out in detail the consequences of the particular model. In the electroweak interactions this will, of course, be of crucial importance in the search for the signatures of new physics.

Here we calculate the axial-vector A^3 vertex, see Fig. 12.22 for notation. To order g^3, it is given by the sum of one-loop diagrams with either the fermions or the scalar circulating in the loop. Explicitly we find

$$T^{\mu\nu\rho}(p,k) = \sum_j \left[T_{\psi_j}^{\mu\nu\rho}(p,k) + T_{\psi_j}^{\nu\mu\rho}(k,p)\right] + T_\Phi^{\mu\nu\rho}(p,k) + T_\Phi^{\nu\mu\rho}(k,p) + \\ + 2\left[T_4^{\mu\nu\rho}(p,k) + T_4^{\mu\rho\nu}(p,-p-k) + T_4^{\nu\rho\mu}(k,-p-k)\right],$$

where $T_{\psi_j}^{\mu\nu\rho}$ denote the fermion triangle loops, $T_\Phi^{\mu\nu\rho}$ the analogous scalar loops, and $T_4^{\mu\nu\rho}$ the scalar loops with the insertion of the vertex $\phi^\dagger\phi A^\mu A_\mu$.

We do not write down the lengthy explicit expression for $T^{\mu\nu\rho}(p,k)$. It cannot be calculated analytically anyway since the self-energies Σ_j and Π have been computed only numerically. (In fact, in our approximation the scalar loops do not contribute.)

The A^3 vertex can, however, be determined analytically in the special case when the external gauge bosons are on-shell i.e., $p^2 = k^2 = q^2 = m_A^2$ and the fermion self-energies are set constant, $\Sigma_j(p^2) = m_j$. It is then found that

$$iT^{\mu\nu\rho}(p,k) = G\left[(q^\mu k^\alpha - k^\mu q^\alpha)p^\beta \epsilon^{\nu\rho}{}_{\alpha\beta} + (p^\nu q^\alpha - q^\nu p^\alpha)k^\beta \epsilon^{\rho\mu}{}_{\alpha\beta} + (k^\rho p^\alpha - p^\rho k^\alpha)q^\beta \epsilon^{\mu\nu}{}_{\alpha\beta}\right]. \tag{12.44}$$

The effective coupling constant G is expressed as $G = -g^3 \sum_{j=1,2}(-1)^j f(m_j^2, m_A^2)$, where

$$f(x,y) = \frac{2}{\pi^2 y}\int_0^1 dz \frac{z(1-z)}{\sqrt{z(3z-4)+\frac{4x}{y}-i\epsilon}} \arctan \frac{z}{\sqrt{z(3z-4)+\frac{4x}{y}-i\epsilon}}.$$

For very small coupling g the gauge boson mass is small as well and the value $f(m^2,0) = 1/24\pi^2 m^2$ is then of particular interest. Note also that the A^3 vertex (12.44) may be obtained from the effective Lagrangian

$$\mathcal{L}_{\text{eff}} = G\epsilon_{\alpha\beta\gamma\delta}(\partial_\sigma A^\alpha)(\partial^\beta A^\sigma)(\partial^\gamma A^\delta).$$

12.7.4 Conclusions

In the framework of a simple Abelian model we have shown that a sufficiently strong Yukawa interaction may induce the spontaneous breakdown of the chiral symmetry. Our ultimate goal is, however, to apply this idea to the gauge theory of electroweak interactions. The upcoming LHC machine at CERN is going to explore the new physics underlying the electroweak symmetry breaking and we hope that our proposal might provide a reasonable alternative to the existing models.

Our hope is based on the following observations. First, with the elementary scalars kept in the Lagrangian one explicitly breaks the interfamily symmetries. Models without scalars struggle with guaranteeing unobservability of physical consequences of these unwanted symmetries. Further, our numerical results suggest that, unlike in the Higgs mechanism, we are able to generate the huge hierarchy of fermion masses without introducing vastly different Yukawa couplings. Another notable fact is that the gauge boson masses are tied to the fermion spectrum in terms of sum rules.

To date, the most serious obstacle to a direct application of the present mechanism to the electroweak interactions is its nonperturbative nature. We have already shown that the scalar spectrum may be adapted to fit the symmetries of the standard model [163]. On the other hand, much work is still in order to make phenomenological predictions that could be compared with experiment. Not only the flavour structure of the standard model makes the set of coupled equations to be solved much larger and thus more complicated, but also the approximations used here to generate the Schwinger–Dyson equations have to be revised. Nevertheless, we are convinced that our goal is worthy of the effort required by this task.

REFERENCES

[1] S. Weinberg, Phys. Rev. **D19**, 1277 (1979).

[2] L. Susskind, Phys. Rev. **D20**, 2619 (1979).

[3] C. T. Hill and E. H. Simmons, Phys. Rep. **381**, 235 (2003), [hep-ph/0203079], erratum ibid 390:553-554, 2004.

[4] K. Lane, hep-ph/0202255.

[5] M. E. Peskin and T. Takeuchi, Phys. Rev. **D46**, 381 (1992).

[6] R. S. Chivukula, B. A. Dobrescu, H. Georgi and C. T. Hill, Phys. Rev. **D59**, 075003 (1999), [hep-ph/9809470].

[7] B. A. Dobrescu, Phys. Rev. **D63**, 015004 (2001), [hep-ph/9908391].

[8] F. Sannino and K. Tuominen, Phys. Rev. **D71**, 051901 (2005), [hep-ph/0405209].

[9] D. K. Hong, S. D. H. Hsu and F. Sannino, Phys. Lett. **B597**, 89 (2004), [hep-ph/0406200].

[10] D. D. Dietrich, F. Sannino and K. Tuominen, Phys. Rev. **D72**, 055001 (2005), [hep-ph/0505059].

[11] S. Dimopoulos and J. Preskill, Nucl. Phys. **B199**, 206 (1982).

[12] N. Arkani-Hamed, A. G. Cohen and H. Georgi, Phys. Lett. **B513**, 232 (2001), [hep-ph/0105239].

[13] F. Sannino and J. Schechter, Phys. Rev. **D52**, 96 (1995), [hep-ph/9501417].

[14] D. Black, A. H. Fariborz, F. Sannino and J. Schechter, Phys. Rev. **D59**, 074026 (1999), [hep-ph/9808415].

[15] R. L. Jaffe, Phys. Rev. **D15**, 267 (1977).

[16] R. L. Jaffe, Phys. Rev. **D15**, 281 (1977).

[17] M. Harada, F. Sannino and J. Schechter, Phys. Rev. **D69**, 034005 (2004), [hep-ph/0309206].

[18] E. Eichten and K. D. Lane, Phys. Lett. **B90**, 125 (1980).

[19] T. Appelquist, M. Piai and R. Shrock, Phys. Rev. **D69**, 015002 (2004), [hep-ph/0308061].

[20] B. Holdom, Phys. Rev. **D24**, 1441 (1981).

[21] K. Yamawaki, M. Bando and K.-i. Matumoto, Phys. Rev. Lett. **56**, 1335 (1986).

[22] T. W. Appelquist, D. Karabali and L. C. R. Wijewardhana, Phys. Rev. Lett. **57**, 957 (1986).

[23] V. A. Miransky and K. Yamawaki, Phys. Rev. **D55**, 5051 (1997), [hep-th/9611142].

[24] J. M. Frere, Phys. Rev. **D35**, 2625 (1987).

[25] R. S. Chivukula, E. H. Simmons and J. Terning, Phys. Lett. **B331**, 383 (1994), [hep-ph/9404209].

[26] C. T. Hill, Phys. Lett. **B266**, 419 (1991).

[27] C. T. Hill, Phys. Lett. **B345**, 483 (1995), [hep-ph/9411426].

[28] T. Appelquist, J. Terning and L. C. R. Wijewardhana, Phys. Rev. Lett. **77**, 1214 (1996), [hep-ph/9602385].

[29] F. Sannino and J. Schechter, Phys. Rev. **D60**, 056004 (1999), [hep-ph/9903359].

[30] H. Gies and J. Jaeckel, hep-ph/0507171.

[31] F. N. Ndili, hep-ph/0508111.

[32] T. Appelquist and F. Sannino, Phys. Rev. **D59**, 067702 (1999), [hep-ph/9806409].

[33] T. Appelquist, P. S. Rodrigues da Silva and F. Sannino, Phys. Rev. **D60**, 116007 (1999), [hep-ph/9906555].

[34] R. Sundrum and S. D. H. Hsu, Nucl. Phys. **B391**, 127 (1993), [hep-ph/9206225].

[35] N. Evans and F. Sannino, hep-ph/0512080.

[36] K. D. Lane and E. Eichten, Phys. Lett. **B222**, 274 (1989).

[37] K. D. Lane and M. V. Ramana, Phys. Rev. **D44**, 2678 (1991).

[38] E. Corrigan and P. Ramond, Phys. Lett. **B87**, 73 (1979).

[39] ALEPH, DELPHI, L3, OPAL, SLD, LEP Electroweak Working Group, SLD Electroweak Group, and SLD Heavy Flavour Group, hep-ex/0509008.

[40] D. D. Dietrich, F. Sannino and K. Tuominen, Phys. Rev. **D73**, 037701 (2006), [hep-ph/0510217].

[41] H.-J. He, C. T. Hill and T. M. P. Tait, Phys. Rev. **D65**, 055006 (2002), [hep-ph/0108041].

[42] N. D. Christensen and R. Shrock, Phys. Lett. **B632**, 92 (2006), [hep-ph/0509109].

[43] T. Appelquist and R. Shrock, Phys. Lett. **B548**, 204 (2002), [hep-ph/0204141].

[44] T. Appelquist, N. Christensen, M. Piai and R. Shrock, Phys. Rev. **D70**, 093010 (2004), [hep-ph/0409035].

[45] V. A. Miransky, M. Tanabashi and K. Yamawaki, Phys. Lett. **B221**, 177 (1989).

[46] V. A. Miransky, M. Tanabashi and K. Yamawaki, Mod. Phys. Lett. **A4**, 1043 (1989).

[47] W. J. Marciano, Phys. Rev. Lett. **62**, 2793 (1989).

[48] Y. Nambu, EFI-89-08.

[49] W. A. Bardeen, C. T. Hill and M. Lindner, Phys. Rev. **D41**, 1647 (1990).

[50] B. A. Dobrescu and C. T. Hill, Phys. Rev. Lett. **81**, 2634 (1998), [hep-ph/9712319].

[51] S. Eidelman *et al.,* Eds. (Particle Data Group), Review of Particle Physics, Phys. Lett. **B592** 1 (2004).

[52] K. Lane and S. Mrenna, Phys. Rev. **D67**, 115011 (2003), [hep-ph/0210299].
[53] K. D. Lane, Phys. Rev. **D60**, 075007 (1999), [hep-ph/9903369].
[54] K. D. Lane, hep-ph/9903372.
[55] J. Abdallah *et al.* (DELPHI Collaboration), Eur. Phys. J. **C22**, 17 (2001), [hep-ex/0110056].
[56] N. Gollub, DESY-THESIS-2001-063.
[57] N. Meyer, DESY-THESIS-2005-001.
[58] OPAL Collaboration, PN485, July 2001.
[59] F. Abe *et al.* (CDF Collaboration), Phys. Rev. Lett. **82**, 3206 (1999).
[60] T. Affolder *et al.* (CDF Collaboration), Phys. Rev. Lett. **85**, 2056 (2000), [hep-ex/0004003].
[61] F. Abe *et al.* (CDF Collaboration), Phys. Rev. **D55**, 5263 (1997), [hep-ex/9702004].
[62] F. Abe *et al.* (CDF Collaboration), Phys. Rev. Lett. **82**, 2038 (1999), [hep-ex/9809022].
[63] A. R. Zerwekh and R. Rosenfeld, Phys. Lett. **B503**, 325 (2001), [hep-ph/0103159].
[64] R. Sekhar Chivukula, A. Grant and E. H. Simmons, Phys. Lett. **B521**, 239 (2001), [hep-ph/0109029].
[65] A. R. Zerwekh, hep-ph/0603094.
[66] T. Affolder *et al.* (CDF Collaboration), Phys. Rev. Lett. **84**, 1110 (2000).
[67] F. Abe *et al.* (CDF Collaboration), Phys. Rev. Lett. **83**, 3124 (1999), [hep-ex/9810031].
[68] L. Feligioni, Int. J. Mod. Phys. **A20**, 3302 (2005).
[69] V. M. Abazov *et al.* (D0 Collaboration), Phys. Rev. Lett. **87**, 061802 (2001), [hep-ex/0102048].
[70] D0 Collaboration, D0note 4561-Conf, v1.2 .
[71] ATLAS Collaboration, CERN/LHCC/99-14 .
[72] G. Azuelos, R. Mazini and S. R. Slabospitsky, ATLAS note ATL-PHYS-99-021.
[73] T. Han, Y. J. Kim, A. Likhoded and G. Valencia, Nucl. Phys. **B593**, 415 (2001), [hep-ph/0005306].
[74] J. A. Aguilar-Saavedra *et al.* (ECFA/DESY LC Physics Working Group), hep-ph/0106315.
[75] G. Weiglein *et al.* (LHC/LC Study Group), hep-ph/0410364.
[76] R. Casalbuoni *et al.*, Z. Phys. **C60**, 315 (1993), [hep-ph/9303201].
[77] R. Casalbuoni *et al.*, Phys. Rev. **D53**, 5201 (1996), [hep-ph/9510431].
[78] A. R. Zerwekh, hep-ph/0512261.
[79] A. Belyaev, A. Blum, R. S. Chivukula and E. H. Simmons, hep-ph/0506086.
[80] D0 Collaboration, D0 note 4880-CONF, Aug. 2005.
[81] V. Necula, Search for a new resonance decaying into $t\bar{t}$, talk at the Particles and Nuclei International Conference 2005 (PANIC05), Santa Fe, New Mexico, 24-28 October 2005
Available at `http://panic05.lanl.gov/abstracts/234/PANIC_ValentinNEcula_234.pdf`.
[82] S. Dimopoulos and L. Susskind, Nucl. Phys. **B155**, 237 (1979).
[83] M. Soldate, M. H. Reno and C. T. Hill, Phys. Lett. **B179**, 95 (1986).
[84] J. Chay and E. H. Simmons, Nucl. Phys. **B315**, 541 (1989).
[85] H. Georgi, Nucl. Phys. **B307**, 365 (1988).
[86] H. Georgi, Phys. Lett. **B216**, 155 (1989).
[87] S. F. King, Phys. Lett. **B229**, 253 (1989).
[88] H. Georgi, Nucl. Phys. **B416**, 699 (1994), [hep-ph/9209244].
[89] L. Randall, Nucl. Phys. **B403**, 122 (1993), [hep-ph/9210231].
[90] T. Appelquist and N. J. Evans, Phys. Rev. **D53**, 2789 (1996), [hep-ph/9509270].
[91] T. Appelquist and R. Shrock, Phys. Rev. Lett. **90**, 201801 (2003), [hep-ph/0301108].

[92] J. C. Pati and A. Salam, Phys. Rev. **D10**, 275 (1974).
[93] S. Raby, S. Dimopoulos and L. Susskind, Nucl. Phys. **B169**, 373 (1980).
[94] B. Holdom, Phys. Rev. **D23**, 1637 (1981).
[95] S. P. Martin, Nucl. Phys. **B398**, 359 (1993), [hep-ph/9211292].
[96] T. Appelquist and J. Terning, Phys. Rev. **D50**, 2116 (1994), [hep-ph/9311320].
[97] S. Dimopoulos and J. R. Ellis, Nucl. Phys. **B182**, 505 (1982).
[98] Y. Nagoshi and K. Nakanishi, Phys. Rev. **D52**, 4143 (1995), [hep-ph/9503274].
[99] A. Martin and K. Lane, Phys. Rev. **D71**, 015011 (2005), [hep-ph/0404107].
[100] R. S. Chivukula, E. H. Simmons and J. Terning, Phys. Rev. **D53**, 5258 (1996), [hep-ph/9506427].
[101] R. S. Chivukula, B. A. Dobrescu and E. H. Simmons, Phys. Lett. **B401**, 74 (1997), [hep-ph/9702416].
[102] S.-C. Chao and K. D. Lane, Phys. Lett. **B159**, 135 (1985).
[103] R. S. Chivukula, B. A. Dobrescu and J. Terning, Phys. Lett. **B353**, 289 (1995), [hep-ph/9503203].
[104] T. Appelquist, N. J. Evans and S. B. Selipsky, Phys. Lett. **B374**, 145 (1996), [hep-ph/9601305].
[105] R. S. Chivukula, S. B. Selipsky and E. H. Simmons, Phys. Rev. Lett. **69**, 575 (1992), [hep-ph/9204214].
[106] T. Appelquist, M. Einhorn, T. Takeuchi and L. C. R. Wijewardhana, Phys. Lett. **B220**, 223 (1989).
[107] S. F. King and D. A. Ross, Phys. Lett. **B236**, 327 (1990).
[108] N. J. Evans, Phys. Lett. **B331**, 378 (1994), [hep-ph/9403318].
[109] P. Arnold and C. Wendt, Phys. Rev. **D33**, 1873 (1986).
[110] G. Burdman, R. S. Chivukula and N. J. Evans, Phys. Rev. **D61**, 035009 (2000), [hep-ph/9906292].
[111] G. Burdman, R. S. Chivukula and N. J. Evans, Phys. Rev. **D62**, 075007 (2000), [hep-ph/0005098].
[112] F. Sannino, Int. J. Mod. Phys. **A20**, 6133 (2005), [hep-ph/0506205].
[113] D. D. Dietrich, To appear in the proceedings of 18th International Conference on Ultrarelativistic Nucleus–Nucleus Collisions: Quark Matter 2005 (QM 2005), Budapest, Hungary, 4–9 Aug. 2005.
[114] A. G. Cohen and H. Georgi, Nucl. Phys. **B314**, 7 (1989).
[115] T. Appelquist, K. D. Lane and U. Mahanta, Phys. Rev. Lett. **61**, 1553 (1988).
[116] T. Appelquist, J. Terning and L. C. R. Wijewardhana, Phys. Rev. **D44**, 871 (1991).
[117] R. S. Chivukula, Phys. Rev. **D55**, 5238 (1997), [hep-ph/9612267].
[118] E. Witten, Phys. Lett. **B117**, 324 (1982).
[119] M. E. Peskin and T. Takeuchi, Phys. Rev. Lett. **65**, 964 (1990).
[120] Z. P. Duan, P. S. Rodrigues da Silva and F. Sannino, Nucl. Phys. **B592**, 371 (2001), [hep-ph/0001303].
[121] M. Harada, M. Kurachi and K. Yamawaki, hep-ph/0509193.
[122] D. K. Hong and H.-U. Yee, hep-ph/0602177.
[123] S. Dutta, K. Hagiwara and Q.-S. Yan, hep-ph/0603038.
[124] Q.-S. Yan, private communication.
[125] S. F. King, Phys. Rev. **D45**, 990 (1992).
[126] G. Burdman and N. J. Evans, Phys. Rev. **D59**, 115005 (1999), [hep-ph/9811357].
[127] S. B. Gudnason, C. Kouvaris and F. Sannino, hep-ph/0603014.
[128] K. Tuominen, private communication.
[129] S. Nussinov, Phys. Lett. **B165**, 55 (1985).
[130] D. S. Akerib *et al.* (CDMS Collaboration), Phys. Rev. Lett. **96**, 011302 (2006), [astro-ph/0509259].

[131] C.-P. Ma and E. Bertschinger, Astrophys. J. **612**, 28 (2004), [astro-ph/0311049].
[132] O. Lahav and A. R. Liddle, astro-ph/0601168.
[133] J. Bagnasco, M. Dine and S. D. Thomas, Phys. Lett. **B320**, 99 (1994), [hep-ph/9310290].
[134] V. A. Kuzmin, V. A. Rubakov and M. E. Shaposhnikov, Phys. Lett. **B155**, 36 (1985).
[135] S. M. Barr, R. S. Chivukula and E. Farhi, Phys. Lett. **B241**, 387 (1990).
[136] J. A. Harvey and M. S. Turner, Phys. Rev. **D42**, 3344 (1990).
[137] S. B. Gudnason, C. Kouvaris and F. Sannino, in preparation.
[138] D. Dominici, Riv. Nuovo Cim. **20**, 1 (1997), [hep-ph/9711385].
[139] H. B. O'Connell, B. C. Pearce, A. W. Thomas and A. G. Williams, Prog. Part. Nucl. Phys. **39**, 201 (1997), [hep-ph/9501251].
[140] A. R. Zerwekh, hep-ph/0307130.
[141] A. Belyaev, T. Han and R. Rosenfeld, JHEP **07**, 021 (2003), [hep-ph/0204210].
[142] D. Cavalli *et al.*, hep-ph/0203056.
[143] S. Mrenna and J. D. Wells, Phys. Rev. **D63**, 015006 (2001), [hep-ph/0001226].
[144] R. Kinnunen, S. Lehti, A. Nikitenko and P. Salmi, J. Phys. **G31**, 71 (2005), [hep-ph/0503067].
[145] S. Weinberg, Phys. Rev. **D13**, 974 (1976).
[146] E. Farhi and L. Susskind, Phys. Rep. **74**, 277 (1981).
[147] R. Casalbuoni *et al.*, Nucl. Phys. **B555**, 3 (1999), [hep-ph/9809523].
[148] A. Belyaev, A. Blum, R. S. Chivukula and E. H. Simmons, Phys. Rev. **D72**, 055022 (2005), [hep-ph/0506086].
[149] M. Carena, S. Mrenna and C. E. M. Wagner, Phys. Rev. **D60**, 075010 (1999), [hep-ph/9808312].
[150] M. Carena, S. Mrenna and C. E. M. Wagner, Phys. Rev. **D62**, 055008 (2000), [hep-ph/9907422].
[151] S. Dawson, A. Djouadi and M. Spira, Phys. Rev. Lett. **77**, 16 (1996), [hep-ph/9603423].
[152] R. V. Harlander and M. Steinhauser, Phys. Lett. **B574**, 258 (2003), [hep-ph/0307346].
[153] R. V. Harlander and M. Steinhauser, Phys. Rev. **D68**, 111701 (2003), [hep-ph/0308210].
[154] R. V. Harlander and M. Steinhauser, JHEP **09**, 066 (2004), [hep-ph/0409010].
[155] S. Dimopoulos, S. Raby and G. L. Kane, Nucl. Phys. **B182**, 77 (1981).
[156] J. R. Ellis, M. K. Gaillard, D. V. Nanopoulos and P. Sikivie, Nucl. Phys. **B182**, 529 (1981).
[157] B. Holdom, Phys. Rev. **D24**, 157 (1981).
[158] M. Spira, Nucl. Instrum. Methods **A389**, 357 (1997), [hep-ph/9610350].
[159] T. Brauner and J. Hošek, Phys. Rev. **D72**, 045007 (2005), [hep-ph/0505231].
[160] J. S. Schwinger, Phys. Rev. **125**, 397 (1962).
[161] R. Jackiw and K. Johnson, Phys. Rev. **D8**, 2386 (1973).
[162] J. Hošek, Phys. Rev. **D36**, 2093 (1987).
[163] T. Brauner and J. Hošek, hep-ph/0407339.